APPLICATIONS OF TWO-DIMENSIONAL QCD

By J. Ellis

CERN — Geneva*

(Presented at the XVII Cracow School of Theoretical Physics, Zakopane, May 27 — June 9, 1977)

The phenomenology to be tested in two-dimensional QCD is first reviewed and 't Hooft's light-like gauge formulation of two-dimensional QCD in the $1/N_{\text{colour}}$ expansion developed. Then, the model is applied to a number of hadronic reactions involving electromagnetic currents and also to some purely hadronic interactions.

1. Introduction

It has been said that Quantum Chromodynamics (QCD) is the first field theory of the strong interactions which is not obviously wrong [1]. Unfortunately, this does not necessarily mean that QCD is actually right. Even the derivation and applications of the much-cherished property of asymptotic freedom [2] completely ignore [3] the confinement problem, and no-one has yet proved that QCD confines quarks. On the other hand, QCD is generally believed to be consistent with, or indeed imply, many of the ideas in the folklore of present-day strong interaction phenomenology. This latter may be divided into four general categories:

(*i*) Spectroscopy.

(*ii*) Asymptotic freedom, relevant to some processes known to be controlled by dynamics at short distances. These include deep inelastic reactions such as $e^+e^- \to \gamma^* \to$ hadrons and e + hadron $\to$ e′ + anything.

(*iii*) "Hard" Processes, where large momentum transfers are involved, but a direct connection with dynamics at short distance and asymptotic freedom has not been established. Such processes include lepton-pair production in hadron-hadron collisions, quasi-elastic form factors and large-angle scattering, and particle production at large p_T in hadron-hadron collisions.

(*iv*) "Soft" Processes, where only small momentum transfers are involved, and no-one would believe that short-distance dynamics plays an essential role. Such processes include hadron-hadron scattering at small momentum transfers, total cross-sections and particle production at small p_T in hadron-hadron collisions.

* Address: CERN, CH-1211 Geneva 23, Switzerland.

Unfortunately, our understanding [4] of four-dimensional QCD (QCD_4) is too primitive for making profound studies of many of these aspects of strong interactions.

So we must fall back on models, and the purpose of these lectures is to develop and use two-dimensional QCD (QCD_2) [5] as a tool for investigating our phenomenological ideas about QCD_4. Clearly QCD_2 must be used with care — it has no transverse size or momenta, the infra-red and confinement structure must be very different from QCD_4, and so on. The hope is nevertheless to convince you that QCD_2

— is a simple and tractable model suitable for studying the interactions of confined quarks,

— has useful things to say about the validity of many common ideas in strong interaction phenomenology, and

— may suggest some new ideas suitable for phenomenological tests in the real four-dimensional world.

In this first lecture, the phenomenological ideas we might want to test in QCD_2 are briefly reviewed, 't Hooft's light-like gauge formulation [5] of QCD_2 in the $1/N_{\text{colour}}$ expansion is developed, and finally some spectroscopic topics are discussed. In the second lecture the model is applied [7—9] to a number of hadronic reactions involving electromagnetic currents. The third lecture looks at some purely hadronic interactions [10–13] and tries to draw some conclusions.

1.1. Phenomenological ideas to be tested

Spectroscopy

Any list of prominent features of hadron spectroscopy must start with the absence [14] of quarks. The confinement mechanism which removes them from the physical spectrum is surely very different in QCD_2 from what it may be in QCD_4. In two dimensions gluon exchange gives a linearly rising potential, whereas in four dimensions one gluon exchange (OGLE) gives a $1/r$ potential, no clear signs of confinement appear in perturbation theory [15], and it seems that some non-perturbative mechanism [16] must be invoked. It is hoped this will give an effectively potential which rises linearly at large distances. The observed linearly rising ($J \propto M^2$) Regge trajectories of mesons seem to require such a phenomenon, which is often associated with a string-like [17] structure connecting quark and antiquark. The observed Regge trajectories seem to group themselves so that mesons and baryons form multiplets of $SU(2N_f)$, where N_f is the number of quark flavours, and 2 is the number of quark spin states. Testing this symmetry seems difficult in two dimensions where there is no spin!

We also have ideas about what happens in the limits of light and heavy quarks. As $m_q \to 0$, we believe the strong interactions develop an $SU(N_f) \times SU(N_f)$ symmetry which is realized by pseudoscalar Goldstone bosons (chiral symmetry) [18]. As $m_{u,d,s} \to 0$ we expect

$$m_{\pi^\pm}^2 \approx \mu(m_u + m_d) \to 0,$$

$$m_{K^\pm}^2 \approx \mu(m_u + m_s) \to 0, \tag{1.1}$$

where μ is some typically hadronic mass scale. The π^0 mass should also vanish analogously to (1.1), but there is a subtlety about the η and η' which we do not understand [19]. If you believe that $m_s \lesssim 500$ MeV in the real world, then (1.1) and $m_\pi^2/m_K^2 \approx 1/25$ imply that $m_{u,d}$ are only a few MeV each. A corollary of chiral symmetry is the Adler zero condition that pion (kaon) amplitudes should vanish [20] as $p_\mu^{\pi(K)} \to 0$. The property (1.1) does not hold in many bag models or strong coupling approximations for studying quark confinement on a lattice [21].

It has been suggested that as $m_q \to \infty$ the lightest $q\bar{q}$ mesons may be approximately non-relativistic bound states in a simple Coulomb potential ("charmonium") [22]. Furthermore, electromagnetic and strong transitions between these states may have simple descriptions [22, 23] in terms of quark-gluon bound state perturbation theory.

Asymptotic freedom

There is a class of hadronic processes involving very virtual photons at high energies which are believed to be related to the short-distance and light-cone singularities underlying strong interactions [2, 24]. An example is $(e^-e^+ \to \gamma^* \to \text{hadrons})$, which is proportional to

$$\pi(q^2) \equiv \int d^4x e^{iq\cdot x} \langle 0| [J_\mu^{em}(x), J^{\mu em}(0)] |0\rangle. \tag{1.2}$$

As $q^2 \to +\infty$, $q_0 \to \infty$ in the centre-of-mass system so that the exponential in (1.2) picks out $x_0 \to 0$, which implies $x_\mu \to 0$ because the commutator is causal. Consider also deep inelastic lepton-hadron processes ($e+H \to e+X$, $\nu+H \to \mu+X$, $\nu+H \to \nu+X$, etc.). In the Bjorken limit

$$Q^2 \equiv -q^2 \to \infty, \quad \nu \equiv p\cdot q \to \infty, \quad X_{Bj} \equiv \frac{Q^2}{2p\cdot q} \text{ fixed}, \tag{1.3}$$

the $x^2 \to 0$ light-cone singularity between two hadronic electromagnetic currents is picked out. Cross-sections for these deep inelastic processes are conventionally calculated using asymptotic freedom, and assuming that the long-distance non-perturbative confinement mechanism can be ignored, so that the hadronic cross-sections are "as if" quarks were

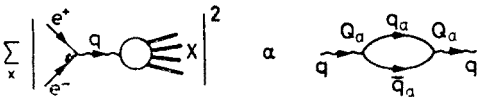

Fig. 1. e^+e^- annihilation into hadrons given by the parton model motivated by asymptotic freedom

essentially free. It is not at all clear that these "as if" calculations — which can only be understood in the sense of averaging over hadronic resonance peaks — are in fact legitimate. Be that as it may, "as if" calculations yield the parton [25] results (from Fig. 1)

$$\frac{\sigma(e^+e^- \to \gamma^* \to \text{hadrons})}{\sigma(e^+e^- \to \gamma^* \to \mu^+\mu^-)} \xrightarrow{Q^2\to\infty} N_c \sum_{\substack{\text{quark}\\ \text{charges}}} Q_q^2 \tag{1.4}$$

and (from Fig. 2)

$$\nu W_2(e+H \to e'+X) \to \sum_{Bj} \sum_{quarks} Q_q^2 X_{Bj} P_q(X_{Bj}), \tag{1.5}$$

where $P_q(X_{Bj})$ is the probability of finding a quark q with infinite momentum fraction X_{Bj} inside the hadron target H. (The formula is modified by logarithmic factors in QCD_4,

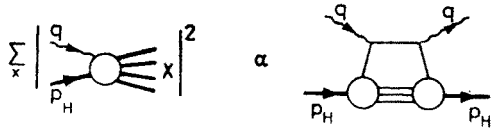

Fig. 2. $\sigma(e+H \to e+X)$ given by the parton model motivated by asymptotic freedom

but these do not alter the essential picture.) A related idea, which is not purely a short-distance property but relates also to the long-range confinement problem, is the suggestion

Fig. 3. Quark fragmentation model for $\sigma(e^+e^- \to M+X)$

an "asymptotically free" quark produced in either of the deep inelastic reactions (1.4), (1.5) should fragment into hadrons through a universal function (see Fig. 3)

$$D_{q \to M}(X_F) : X_F \equiv \frac{p_M}{p_q} \tag{1.6}$$

with p_M and p_q measured in a suitable infinite momentum frame.

"Hard" processes

In this category one may include a number of processes which involve large momentum transfers (Q^2 or t), but where no connection with the underlying short-distance behaviour of the theory has been proved. An example involving large Q^2 currents is the process $H_1+H_2 \to l^+l^-+X$, to which Drell and Yan [26] applied the simple parton-antiparton annihilation model of Fig. 4 to get

$$\frac{d\sigma}{dQ^2}(H_1+H_2 \to l^+l^-(Q^2)+X) = \frac{4\pi\alpha^2}{3N_c Q^4}$$

$$\times \int dX_1 dX_2 \delta\left(X_1 X_2 - \frac{Q^2}{s}\right) \sum_q [P_q(X_1)P_{\bar{q}}(X_2)+P_q(X_2)P_{\bar{q}}(X_1)]X_1 X_2 \tag{1.7}$$

where $P_q(X)$ and $P_{\bar{q}}(X)$ are the same probability densities appearing in (1.5). Other "hard" processes include quasi-elastic electromagnetic form factors of hadrons, large angle elastic hadron-hadron scattering, and inclusive particle production at large p_T. Many people

[27, 28] have proposed parton or constituent interchange models for these interactions. Common features are a "hard" subreaction calculated in perturbation theory (cf., $e+q \to e+q$ in deep inelastic scattering) which is embedded in external hadrons using quark probability densities $P_q(X_{Bj})$ [cf. (1.5)] and fragmentation functions $D_{q\to M}(X_F)$

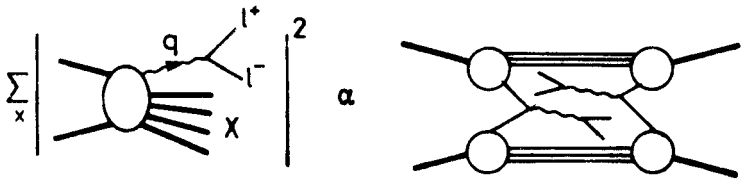

Fig. 4. Lepton-pair production and the Drell–Yan [26] $q\bar{q}$ annihilation model

[cf. (1.6)]. Different "hard" processes are inter-related because the "hard" (short distance) subprocess is believed not to be renormalized by "soft" (long distance) effects [28]. The most fundamental predictions of such models are dimensional counting rules [29] which read scaling laws directly off the fundamental subprocess (cf., $1/Q^2$ for $e^+e^- \to \gamma^* \to$ hadrons from $e^+e^- \to \gamma^* \to q\bar{q}$).

"Soft" processes

These include hadronic reactions at low momentum transfers to which no-one would apply asymptotic freedom or short-distance ideas. Examples are hadron-hadron quasi two-body scattering in the Regge limit near the forward direction, total cross-sections and inclusive hadron production at low p_T. A Regge-behaved amplitude for 2–2 scattering looks like

$$A_{2-2} \underset{\substack{s\to\infty \\ t \text{ fixed}}}{\sim} \gamma^R_{11'}(t)\gamma^R_{22'}(t)s^{\alpha_R(t)} \tag{1.8}$$

where the same $\alpha_R(t)$ appears in all reactions with the same quantum numbers exchanged in the t channel, and is a continuation of the crossed-channel $q\bar{q}$ bound state poles $[J = \alpha_R(M^2)]$, and the amplitude (1.8) has crossed-channel factorization. Amplitudes for

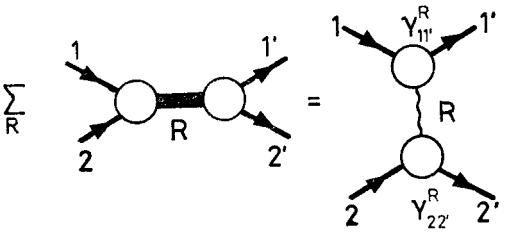

Fig. 5. Direct channel resonances dual to Regge poles

2–3, 2–4, 3–3, etc., scattering should have multi-Regge behaviours generalizing (1.8). Phenomenologically, there is an additional $I = 0$, $C = +1$, Regge singularity near $J = 1$ at $t = 0$ which is not obviously related to crossed channel $q\bar{q}$ bound states — the Pomeron.

Fundamental to the systematization of Regge phenomenology is the dual [30] idea, illustrated in Fig. 5, that

$$\sum \text{direct channel resonances} = \sum \text{crossed channel Regge poles} \tag{1.9}$$

with duality also relating [31] the Pomeron to the production of two or more resonant clusters in the direct channel. If there are just $q\bar{q}$ bound states (no exotics) then duality (1.9) implies the exchange degenerate [32] pattern

$$\alpha_\varrho \approx \alpha_\omega \approx \alpha_f \approx \alpha_{A_2} \tag{1.10}$$

with similar relations for the Regge residues γ^R. Finally, total cross-sections and inclusive hadron distributions at small p_T should be controlled by the same Regge singularities (1.8) with $t = 0$. In particular, the Pomeron would be responsible for Feyman scaling, whereas Regge exchanges would give subasymptotic corrections.

1.2. The $1/N_{\text{colour}}$ expansion

A powerful framework for discussing the above dual ideas for "soft" processes is provided by the $1/N_{\text{colour}}$ [33–35] and related topological expansions [35, 36]. We will see also that the $1/N_c$ expansion plays an essential role [5] in practical calculations with QCD_2. The idea is to consider the limit

$$N_c \to \infty : g^2 N_c \text{ fixed} \tag{1.11}$$

of graphs is QCD. Quarks are represented by fields q_a^i: $i = 1, \ldots, N_c$ and $a = 1, \ldots, N_f$ are colour and flavour indices, respectively, while gluon fields $A_{\mu j}^i$ are written in a matrix

Fig. 6. Notation for quark and gluon propagators in the $1/N_c$ expansion

notation. The notation is indicated in Fig. 6. Since we want to consider an $SU(N_c)$ gauge theory with $N_c^2 - 1$ massless gluons, we must remove the trace component from $A_{\mu j}^i$

$$\tilde{A}_{\mu j}^{\ i} \equiv A_{\mu j}^{\ i} - \frac{1}{N_c} \delta_j^i A_{\mu k}^{\ k} \tag{1.12}$$

which actually makes no difference at leading order in $1/N_c$.

There is a remarkably simple topological classification of QCD diagrams obtained [34, 35] in the limit (1.11). Fig. 7 shows how some low order diagrams for the quark propagator and $q\bar{q}$ scattering can be neglected in the limit: one is just left with planar diagrams. In general, we can imagine drawing any QCD Feynman diagram such that the colour lines do not touch or cross on a complicated surface with H handles and B boundaries. The diagram in the $U(N_c)$ theory then has a multiplicative weight

$$(g^2 N_c)^{\frac{1}{2} V_3 + V_4} N_c^{2-2H-B} \tag{1.13}$$

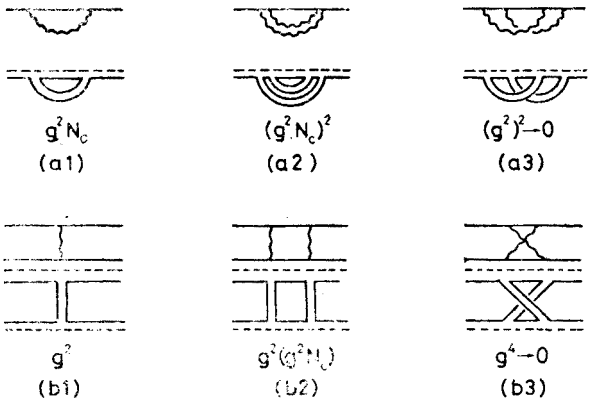

Fig. 7. Some diagrams (a) for the renormalized quark propagator, and (b) for $q\bar{q}$ scattering, showing how some (a_3), (b_3) may be neglected as $N_c \to \infty$

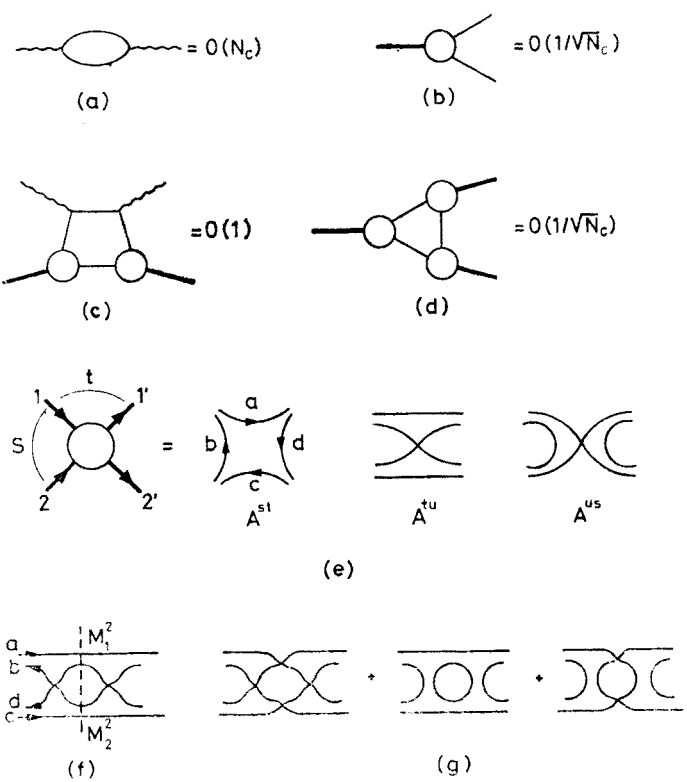

Fig. 8. Counting of powers of N_c for (a) e^+e^- annihilation, (b) meson-$q\bar{q}$ vertex, (c) $e+H \to e+X$, (d) 3-meson vertex, (e) leading $\sigma(1/N_c)$ contributions to meson-meson scattering, (f) and (g) $O(1/N_c^2)$ contributions to meson-meson scattering

where V_3 is the number of $q\bar{q}G$ and 3G vertices, V_4 is the number of 4G vertices. It is not difficult to satisfy oneself of the validity of (1.13) by considering a simple example of each topology, and then adding extra gluon vertices and colour loops à la carte.

Simple examples of N_c counting for some of the physical processes discussed in Section 1.2 are shown in Fig. 8. Notice that since mesons are colour singlets, their $q\bar{q}$ wave functions must have a factor $\sqrt{1/N_c}$, and the counting for reactions involving mesons is got by attaching them to external quark boundaries. There is no simple way of treating baryons in the $1/N_c$ expansion [37]. Notice the leading $O(1/N_c)$ diagrams for meson-meson scattering in Fig. 8(e). These diagrams yield simultaneously direct channel meson poles — which are very narrow since

$$\Gamma(M_1 \to M_2 + M_3) = O\left(\frac{1}{N_c}\right) \tag{1.14}$$

— and crossed-channel poles. They therefore yield the duality (1.9). On the other hand the diagram of Fig. 9a has two clusters in the direct channel, and might be expected to yield a bare Pomeron [31] .What happens in the crossed channel? Topologically, a cylinder

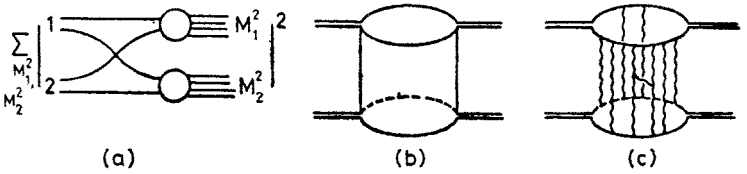

Fig. 9. (a) Absorptive part of Fig. 9(f), and (b) representation as cylinder exchange, which might (c) be due to multiple gluon exchange

is exchanged (see Fig. 9b), and consistency of dual resonance models [38] requires that the cylinder have particle poles. In QCD language, these would be bound states of gluons (see Fig. 9c) (gluonium) which should be very narrow [35]:

$$\Gamma(\text{Gluonium} \to M_1(q\bar{q}) + M_2(q\bar{q})) = O\left(\frac{1}{N_c^2}\right). \tag{1.15}$$

Whether these things exist and are observable is completely unkown [39].

It should be emphasized [35] that you can always add closed quark loops into any diagram — see Fig. 10 — at the expense (1.13) of a factor (N_f/N_c). Such insertions do not

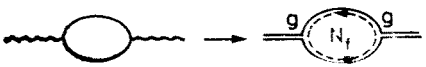

Fig. 10. Insertion of a quark loop introduces a factor N_f/N_c

alter the global topology of the diagram, and Veneziano and others have emphasized the utility of the limit

$$N_f/N_c, \quad g^2 N_c \text{ fixed}; \quad N_c \to \infty \tag{1.16}$$

in which all such insertions are summed: the Topological Expansion. Such diagrams are required by unitarity, but believed not to alter the dual properties (1.9), etc. In QCD_2, work has mainly been devoted to the leading order in N_c for any given topology, and setting up a Topological Expansion is an open and interesting problem.

1.3. The basic formalism of QCD_2

Our basic Lagrangian is [2, 4]

$$\mathscr{L} = \tfrac{1}{4} G_{\mu\nu j}^{\ \ i} G^{\mu\nu j}_{\ \ i} + \bar{q}_i^a (i\gamma D^i_j - m_a \delta^i_j) q_a^j \tag{1.17}$$

where the gluon field strength

$$G_{\mu\nu j}^{\ \ i} \equiv \partial_\mu A_{\nu j}^{\ \ i} - \partial_\nu A_{\mu j}^{\ \ i} + g[A_\mu, A_\nu]^i_j \tag{1.18}$$

and the covariant derivative

$$D_{\mu j}^{\ \ i} \equiv \partial_\mu \delta^i_j + g \tilde{A}_{\mu j}^{\ \ i}, \tag{1.19}$$

with $\tilde{A}_{\mu j}^{\ \ i}$ defined by Eq. (1.12). To analyze (1.17) – (1.19) in two dimensions we will use [5] light-like co-ordinates.

$$x_\pm \equiv \frac{1}{\sqrt{2}}(x_0 \pm x_1) \equiv x^\mp; \quad p_\pm \equiv \frac{1}{\sqrt{2}}(p_0 \pm p_1) \equiv p^\mp, \tag{1.20}$$

so that

$$p \cdot q = p_- q_+ + p_+ q_-$$

and the Dirac γ algebra is particularly simple

$$\gamma_+^2 = \gamma_-^2 = 0; \quad \{\gamma_+, \gamma_-\} = 2; \quad [\gamma_+, \gamma_-] \equiv 2\gamma_5. \tag{1.21}$$

't Hooft used the light-like gauge [40]

$$A_- = \frac{1}{\sqrt{2}}(A_0 - A_1) = 0.$$

In this case (as in all other linear gauges) the multigluon interactions disappear because $[A_\mu, A_\nu] = 0$. The only non-zero component of $G_{\mu\nu j}^{\ \ i}$ (1.18) is then

$$G_{+\ -j}^{\ \ i} = -\partial_- A_{+\ j}^{\ i}. \tag{1.22}$$

The equations of motion of the theory (1.17) are then

$$\delta \bar{q}_a^i \Rightarrow 2i\partial_-[(1-\gamma_5) q_i^a] = m_a \gamma_-[(1+\gamma_5) q_i^a] \tag{1.23}$$

indicating that the left-handed quark field

$$q_L \equiv \left(\frac{1-\gamma_5}{2}\right) q$$

is entirely dependent on the right-handed quark field

$$q_R \equiv \left(\frac{1+\gamma_5}{2}\right) q$$

and

$$\delta A_{+j}^{i} \Rightarrow \partial_-^2 A_{+i}^{j} = -\sqrt{2}\, g q_{Ra}^{+j} q_{Ri}^{a} \tag{1.24}$$

indicating that the gluon field A_+ is also completely dependent on q_R. Thus there are no independent, dynamical, gluonic degrees of freedom, and the only field to quantize is q_R:

$$\{q_R(x_+, x_-), q_R^+(y_+, x_-)\} = \delta(x_+ - y_+)\left(\frac{1+\gamma_5}{2}\right) \tag{1.25}$$

is the canonical light-like quantization condition. The gluons just give a linearly rising Coulomb potential which is instantaneous with respect to the "time" variable x_-. The gluon Green's function which solves

$$\partial_-^2 A_+ = \delta^2(x) \tag{1.26}$$

is just

$$A_+(x_+, x_-) = \delta(x_-)\,(\tfrac{1}{2}|x_+| + Bx_+ + C). \tag{1.27}$$

The parameters B and C reflect residual gauge degrees of freedom which can be removed or ignored. In the calculations described here we will set $B = C = 0$: the momentum space version of (1.27) is then [41]

$$\text{P.V.}\left(\frac{1}{k_-^2}\right) \equiv \tfrac{1}{2}\left[\frac{1}{(k_- - i\varepsilon)^2} + \frac{1}{(k_- + i\varepsilon)^2}\right]. \tag{1.28}$$

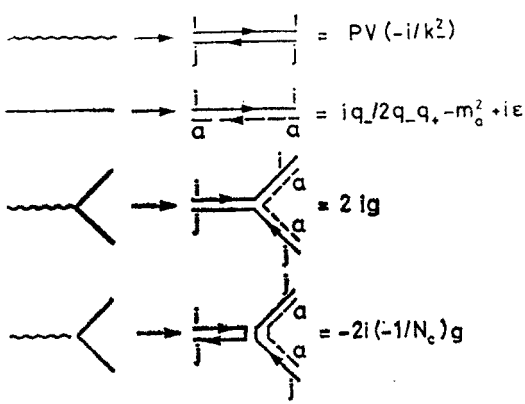

Fig. 11. Feynman graph rules for QCD_2

We are now in a position to write down the Feynman graph rules for QCD_2 (see Fig. 11). Notice that because of the simple 2 dimensional γ algebra (1.21) it is possible to write down the rules without using any γ matrices.

The resulting theory is very similar to QED_2 [6] except that the group theoretical weights (1.13) enforce a different procedure for summing graphs. The first important example is the renormalized quark propagator [5]. Fig. 7 (a3) gives an example of a graph which can be neglected in the $1/N_c \to \infty$ limit. The leading order diagrams can be written as nested rainbows. The simplest such diagram, shown in Fig. 7(a1), has the value

$$7(\mathrm{a1}) = N_c(-2ig)^2 \int \frac{d^2k}{(2\pi)^2}\left(\frac{-i}{k_-^2}\right)\frac{i(p_-+k_-)}{(p+k)^2-m_a^2+i\varepsilon} \tag{1.29}$$

We first do the k_+ integral in (1.29) by introducing a symmetric cut-off Λ:

$$7(\mathrm{a1}) = \lim_{\Lambda\to\infty}\left\{\frac{-2N_c g^2}{(2\pi)^2}\int\frac{dk_-}{k_-^2}\int_{-\Lambda}^{+\Lambda} dk_+ \frac{1}{\left[(p_++k_+)-\dfrac{m_a^2-i\varepsilon}{2(p_-+k_-)}\right]}\right\}. \tag{1.30}$$

Depending on sign (p_-+k_-) the k_+ pole is in the upper or lower $\frac{1}{2}$ plane, and the k_+ integration contour should be closed appropriately to yield

$$\lim_{\Lambda\to\infty}\int_{-\Lambda}^{+\Lambda} dk_+ \frac{1}{\left[(p_++k_+)-\dfrac{m_a^2-i\varepsilon}{2(p_-+k_-)}\right]} = -\pi i \,\mathrm{sign}\,(p_-+k_-)$$

and hence

$$7(\mathrm{a1}) = \frac{g^2N_c i}{2\pi}\int\frac{dk_-}{k_-^2}\,\mathrm{sign}\,(p_-+k_-) = \frac{g^2N_c i}{\pi p_-}. \tag{1.31}$$

When we consider a higher order diagram such as Fig. 7(a2), there is always at least one k_+ integral which is not trying to be logarithmically divergent as in (1.30), so that the integration contour can be closed in such a way as to give $\int dk_+ = 0$. Then the only diagrams contributing to the renormalized quark propagator are sequences of loops as in Fig. 7(a1), and the renormalized quark propagator

$$S^a(p) = \frac{ip_-}{p^2-m_a^2+i\varepsilon} + \left(\frac{ip_-}{p^2-m_a^2+i\varepsilon}\right)\left(\frac{g^2N_c i}{\pi p_-}\right)\left(\frac{ip_-}{p^2-m_a^2+i\varepsilon}\right) + \ldots = \frac{ip_-}{p^2-\tilde{m}_a^2+i\varepsilon}, \tag{1.32}$$

where

$$\tilde{m}_a^2 \equiv m_a^2 - m^2, \qquad m^2 \equiv \frac{g^2N_c}{\pi} \tag{1.33}$$

is a renormalized quark mass. This quark mass shift depends on the gauge choice of C (1.27), and may even be taken to ∞ [42], but the $C = 0$ value (1.33) has a special role, as we see in the next section.

1.4. Bound states

We start off from the colour singlet $q\bar{q}$ T matrix. The planarity enforced by the $1/N_c$ expansion implies that T obeys the equation indicated in Fig. 12, which can be written as

$$iT(q, q'; p) = \frac{ig^2}{(q_- - q'_-)^2} + 4g^2 N_c \int \frac{d^2k}{(2\pi)^2} \frac{S^a(k)S^{\bar{b}}(p-k)}{(k_- - q_-)^2} T(k, q'; p). \tag{1.34}$$

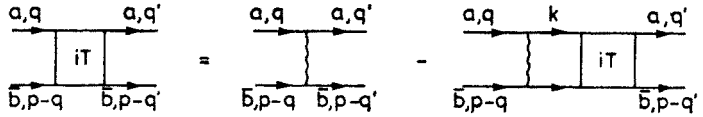

Fig. 12. Equation for the $q\bar{q}$ T-matrix

Suppose that T has a colour singlet bound state meson pole at

$$S \equiv 2p_+p_- \equiv \mu_n^2 m^2, \qquad m^2 = \frac{g^2 N_c}{\pi} \tag{1.35}$$

and sit on it. You will then extract from (1.34) an equation for the meson-$q\bar{q}$ vertex indicated in Fig. 13, and written as

$$\Gamma_n^{a\bar{b}}(q; p) = \frac{-ig^2 N_c}{\pi^2} \int \frac{d^2k}{(k_- - q_-)^2} S^a(k)S^{\bar{b}}(p-k)\Gamma_n^{a\bar{b}}(k; p). \tag{1.36}$$

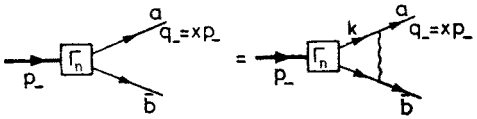

Fig. 13. Equation for the meson $q\bar{q}$ vertex function Γ

It is convenient to rewrite (1.36) by introducing a meson wave function

$$\phi_n^{a\bar{b}}(X) \equiv \frac{i}{\pi} \int_{-\infty}^{\infty} dk_+ S^a(k)S^{\bar{b}}(p-k)\Gamma_n^{a\bar{b}}(k; p) \tag{1.37}$$

where $X \equiv q_-/p_-$ is the light-like momentum fraction carried by the quark. Dimensional analysis implies

$$\Gamma_n^{a\bar{b}}(q; p) = \frac{1}{p_-} \Gamma_n^{a\bar{b}}(X),$$

so that the integration in (1.37) gives

$$\phi_n^{a\bar{b}}(X) = -\frac{1}{m^2} \frac{1}{\left(\mu_n^2 - \dfrac{\gamma_a - 1}{X} - \dfrac{\gamma_b - 1}{1-X}\right)} \Gamma_n^{a\bar{b}}(X), \quad \gamma_a \equiv \frac{m_a^2}{m^2}, \quad \text{for } 0 < X < 1,$$

$$= 0 \qquad \text{for } X < 0, \ X > 1. \tag{1.38}$$

Substituting (1.38) into the integral equation (1.36) gives the 't Hooft [4] bound state wave equation

$$\mu_n^2 \phi_n^{a\bar{b}}(X) = H\phi_n^{a\bar{b}}(X), \tag{1.39a}$$

where $H \equiv H_0 + V$:

$$H_0 = \left(\frac{\gamma_a - 1}{X} + \frac{\gamma_b - 1}{1-X}\right), \quad V = -\int_0^1 \frac{dY}{(X-Y)^2}. \tag{1.39b}$$

The bound state equation (1.39) is formally identical [43] to that for a 2 dimensional string model, but it is unclear how to extend this analogy beyond two dimensions [17].

The solutions to (1.39) have a few formal properties we should discuss before studying the spectroscopic properties. The relevant solutions vanish as

$$\phi_n^{a\bar{b}}(X) \sim \begin{cases} C_n^{a\bar{b}} X^{\beta_a} \\ (-1)^n C_n^{b\bar{a}} (1-X)^{\beta_b} \end{cases} \quad \text{as} \quad \begin{cases} X \to 0 \\ X \to 1, \end{cases} \tag{1.40}$$

where $\beta_a \in (0,1)$ solves the equation

$$\pi\beta_a \cot \pi\beta_a + \gamma_a - 1 = 0 \tag{1.41}$$

and the limiting cases are attained by

$$\beta_a \to \begin{cases} 0 \\ 1 \end{cases} \quad \text{as} \quad m_a \to \begin{cases} 0 \\ \infty. \end{cases} \tag{1.42}$$

The Hamiltonian (1.39b) is Hermitian in the Hilbert space of functions vanishing at the boundaries [5,8], and the wave functions $\phi_n^{a\bar{b}}$; $n = 0,1,2 \ldots$ form a complete orthonormal set:

$$\int_0^1 dX \phi_n^{a\bar{b}}(X)\phi_m^{a\bar{b}}(X) = \delta_{nm}, \tag{1.43a}$$

$$\sum_n \phi_n^{a\bar{b}}(X)\phi_n^{a\bar{b}}(X') = \delta(X-X'). \tag{1.43b}$$

The sequence of bound states n marches off to $m^2 = \infty$, with

$$\Delta m_\infty^2 \equiv \lim_{n\to\infty} (m_{n+1}^2 - m_n^2) = \pi^2 m^2 \tag{1.44}$$

and in the limit they obey a scaling form of (1.39):

$$\phi^a(\xi) = \frac{\gamma_a - 1}{\xi}\phi^a(\xi) - \int_0^\infty d\eta \frac{\phi^a(\eta)}{(\xi-\eta)^2}, \tag{1.45}$$

where

$$\mu_n^2 X \approx \xi,$$

as $n \to \infty$ and

$$\phi_n^{a\bar{b}}(\xi/\mu_n^2) \approx \phi^a(\xi),\ \phi^a(\xi) \approx \begin{cases} \sqrt{2}\sin\left(\dfrac{\xi}{\pi}\right) & \text{as} \quad \xi \to \infty, \\ C_a \xi^{\beta_a} & \text{as} \quad \xi \to 0. \end{cases} \tag{1.46}$$

1.5. Spectroscopic properties

We are now in a position to make a brief comparison with some of the spectroscopic ideas of Section 1.2. The fact that the meson wave function $\phi_n^{a\bar{b}}(X)$ is regular, while the factor

$$\left(\mu_n^2 - \frac{\gamma_a - 1}{X} - \frac{\gamma_b - 1}{1-X}\right)$$

vanishes when the quarks are on mass-shell, implies via (1.38) that the meson-$q\bar{q}$ vertex $\Gamma_n^{a\bar{b}}$ actually vanishes on quark mass-shell [42]. This is a reflection of confinement: we will see more later. The infinite sequence of asymptotically equally spaced states (1.44) is reminiscent of linearly rising Regge trajectories with a universal slope. As shown in Fig. 14,

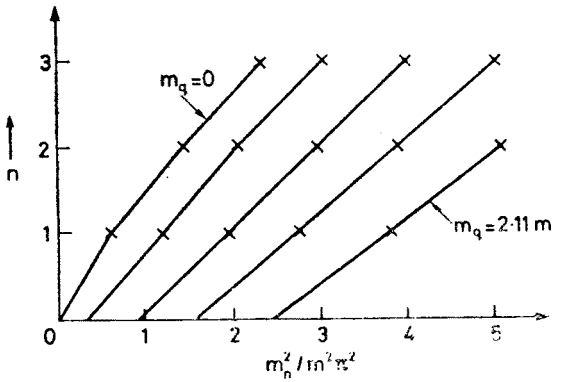

Fig. 14. Spectrum of low-lying mesons for different quark masses, adapted from Ref. [5]

there is a tendency at small n for "trajectories" to steepen for low mass quarks and flatten for high mass quarks.

The lowest lying state made of low-mass quarks actually has $(m_0^{a\bar{b}})^2 \to 0$ as $m_a, m_b \to 0$:

$$(m_0^{a\bar{b}})^2 \approx \left(\frac{m\pi}{\sqrt{3}}\right)(m_a + m_b) \to 0 \tag{1.47}$$

exactly as wanted by chiral symmetry (1.1). If you estimate (see lecture 3)

$$\alpha' \approx 0.9\ \text{GeV}^{-2} \approx \frac{3}{\pi g^2 N_c} = \frac{3}{\pi^2 m^2} \tag{1.48}$$

then you find $m_s \approx 0.2$ GeV, $m_{u,d} \sim 10$ MeV correspond to the 4 dimensional values of m_π^2 and m_K^2. These estimates are in line with other short-distance estimates of quark masses in 4 dimensions [44]. The lowest-lying state also decouples [7, 45, 12] completely from the other mesons as $m_0^2 \to 0$. This may be regarded as a 2 dimensional version of the Adler zero [20], because we see from $p^2 = 2p_+p_-$ that if a 2 dimensional state decouples at $p_\mu = 0$ then it decouples completely, unlike the case in 4 dimensions. This also reflects the theorem [46] that Goldstone bosons per se cannot occur in 2 dimensions.

In the limit as $m_q \to \infty$, Callan, Coote and Gross [7, 47] have found that the equation (1.39) can be approximated by a non-relativistic Schrödinger equation with the two-dimensional version of the Coulomb potential beloved of charmonium proponents. This picture should work for $m_q^2 \gg m^2$, which may well be the case for the charmed quark with a mass of ~ 1.5 GeV. It would be interesting to carry this analysis further, looking to see whether radiative transitions are adequately described by nonrelativistic electric and magnetic dipole transitions, and analyzing Zweig-disallowed decays in more detail than was done by Callan, Coote and Gross [7, 47].

We conclude that, despite its particularities, the spectroscopy of QCD_2 has the right "feel" to it, and in the next lectures we will go on to look at strong interaction dynamics.

2. Hadronic reactions involving currents

2.1. Preliminaries

The main purpose of this lecture is to discuss how currents probe the strong interactions in QCD_2. Some of the processes discussed ($e^+e^- \to \gamma^* \to$ hadrons, $e+M \to e+X$) are a priori strongly believed [24] to probe the short distance and light-cone behaviour of the theory. Others (meson form factors, $M+M \to l^+l^-+X$) [24] are not known to have such a connection with short distances, while yet another ($e^+e^- \to M+X$) probes light-cone behaviour [48] but clearly involves the long-distance confinement problem in an essential way. Before discussing any of these processes in detail, it is necessary to review a few formal aspects of $q\bar{q}$ scattering.

The $q\bar{q}$ T matrix, introduced in Section 1.4 and obeying the integral equation (1.34), can be written [7, 8] as a sum of a one gluon exchange (OGLE) piece, and a multigluon piece which generates meson bound states:

$$T(X \equiv q_-/p_-, X' \equiv q'_-/p'_-; p)$$

$$= \frac{g^2}{p_-^2(X-X')^2} - \frac{g^2}{m^2 p_-^2} \sum_n \frac{1}{p^2 - m_n^2 + i\varepsilon} \Gamma_n^{a\bar{b}}(X)\Gamma_n^{a\bar{b}}(X'), \tag{2.1}$$

where the meson-$q\bar{q}$ vertex $\Gamma_n^{a\bar{b}}$ was introduced in (1.36). Taking the absorptive part of T (2.1) we find [7, 8]

$$\text{Im } T = \frac{g^2\pi}{m^2 p_-^2} \sum_n \delta(p^2 - m_n^2)\Gamma_n^{a\bar{b}}(X)\Gamma_n^{a\bar{b}}(X') \tag{2.2}$$

which has no $q\bar{q}$ continuum, but just meson bound states. Also, from (1.38) we see that

$$\Gamma_n^{a\bar{b}}(X) = -m^2\left(\mu_n^2 - \frac{\gamma_a - 1}{X} - \frac{\gamma_b - 1}{1-X}\right)\phi_n^{a\bar{b}}(X), \tag{2.3}$$

so that as emphasized before, the meson-$q\bar{q}$ vertex $\Gamma_n^{a\bar{b}}$ vanishes when quarks go on mass-shell. There is no trace of a continuum in the colour singlet $q\bar{q}$ channel. It is a simple matter to rewrite the T matrix directly in terms of the meson wave functions $\phi_n^{a\bar{b}}(X)$ when $X, X' \in [0,1]$:

$$T(X, X'; p) = \frac{g^2}{p_-^2}\left(\frac{p^2}{m^2} - \frac{\gamma_a - 1}{X} - \frac{\gamma_b - 1}{1-X}\right)\delta(X - X')$$
$$- \frac{g^2}{p_-^2}\left(\frac{p^2}{m^2} - \frac{\gamma_a - 1}{X} - \frac{\gamma_b - 1}{1-X}\right)\left(\frac{p^2}{m^2} - \frac{\gamma_a - 1}{X'} - \frac{\gamma_b - 1}{1-X'}\right) G(X, X'; p), \tag{2.4}$$

where Green's function G is defined by

$$G(X, X'; p) \equiv \sum_n \frac{\phi_n^{a\bar{b}}(X)\phi_n^{a\bar{b}}(X')}{p^2 - m_n^2 + i\varepsilon}. \tag{2.5}$$

The $\delta(X - X')$ piece in (2.4) will cancel the disconnected part of $q\bar{q}$ scattering leaving behind just the bound state mesons (2.5), as we will now see in some examples.

2.2. e^+e^- annihilation [7, 8]

The cross-section for $e^+e^- \to \gamma^* \to$ hadrons is proportional to the hadronic vacuum polarization indicated in Fig. 15a. To leading order in the $1/N_c$ expansion, the vacuum polarization bubble can be written as a sum over gluon exchanges, as shown in Fig. 15b,

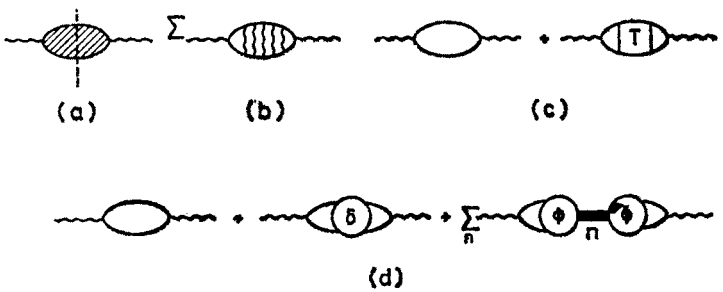

Fig. 15. (a) The absorptive part of the hadronic vacuum polarization, and (b) its representation to leading order in $1/N_c$ as a sum over multi-gluon exchange, which can (c) be written as a sum of disconnected and rescattering pieces, which latter can (d) be decomposed as suggested in equations (2.4, 2.5)

which can be decomposed into a disconnected piece and a piece with a T matrix inserted, as in Fig. 15c. We can in turn use (2.4) to decompose T into the δ function and meson bound state pieces indicated in Fig. 15d. The first diagram in Fig. 15d contains just one

loop integration of the generic form

$$\int \frac{d^2k}{(2\pi)^2} S^a(k)S^{\bar{a}}(q-k) \tag{2.6}$$

which upon integration as in deriving (1.38), is proportional to

$$\int_0^1 dX \frac{1}{\left(\frac{q^2}{m^2} - \frac{\gamma_a - 1}{X} - \frac{\gamma_b - 1}{1-X}\right)}, \tag{2.7}$$

the characteristic energy denominator which appeared also in the numerator of (2.4). If we now study the δ function diagram in Fig. 15d, it clearly has two loop integrations, and has the generic form

$$\int \frac{d^2k}{(2\pi)^2} \int \frac{d^2k'}{(2\pi)^2} S^a(k)S^{\bar{a}}(q-k)\left(\frac{q^2}{m^2} - \frac{\gamma_a - 1}{X} - \frac{\gamma_b - 1}{1-X}\right)\delta(X-X')S^a(k')S^{\bar{a}}(q-k'). \tag{2.8}$$

Performing the k_+ and k'_+ integrals one gets two energy denominators of the form in (2.7):

$$\int dX \int dX' \frac{1}{\left(\frac{q^2}{m^2} - \frac{\gamma_a - 1}{X} - \frac{\gamma_b - 1}{1-X}\right)}\left(\frac{q^2}{m^2} - \frac{\gamma_a - 1}{X} - \frac{\gamma_b - 1}{1-X}\right)$$

$$\times \delta(X-X') \frac{1}{\left(\frac{q^2}{m^2} - \frac{\gamma_a - 1}{X'} - \frac{\gamma_b - 1}{1-X'}\right)}. \tag{2.9}$$

The two contributions (2.7) and (2.9) clearly have the same form: care shows they cancel exactly. Furthermore, evaluating the last diagram in Fig. 15d gives two energy denominators which precisely cancel the two numerators in the G term of (2.4). Thus, if we write the vacuum polarization $\pi_{\mu\nu}(q)$ in the form

$$\pi_{\mu\nu}(q) \equiv (q_\mu q_\nu - q^2 g_{\mu\nu})\bar{\pi}(q^2) \tag{2.10}$$

the remnant of all the cancellations is

$$\bar{\pi}(q^2) = -\frac{Q_a^2 N_c}{\pi} \sum_n \frac{(g_n^a)^2}{(q^2 - m_n^2 + i\varepsilon)}, \qquad g_n^a \equiv \int_0^1 dX \phi_n^{a\bar{a}}(X). \tag{2.11}$$

Notice that no-gluon, OGLE and multigluon exchanges are all crucial participants in the conspiracy to produce this simple result. Many naive parton models [49] do not have this feature, and if taken literally would have physical quarks in the final state.

No trace of the naive quark-parton diagram remains in formula (2.11): how can the "as if" calculation of asymptotic freedom [2, 24] work? We can rewrite (2.11) as

$$\bar{\pi}(q^2) = -\frac{Q_a^2 N_c}{\pi q^2}\left\{\sum_n (g_n^a)^2 + \sum_n \frac{m_n^2 (g_n^a)^2}{q^2 - m_n^2 + i\varepsilon}\right\}. \tag{2.12}$$

If we consider taking $|q^2| \to \infty$ in any direction except along the real axis, then we can ignore the poles in the second term of (2.12) and use the completeness relation (1.43b) to show

$$\sum_n (g_n^a)^2 = \sum_n \int_0^1 dX \phi_n^{a\bar{a}}(X) \int_0^1 dY \phi_n^{a\bar{a}}(Y) = 1,$$

so that the first term in (2.12) is just the quark-parton /asymptotic freedom result

$$\bar{\pi}(q^2) = -\frac{Q_a^2 N_c}{\pi q^2} + \ldots \tag{2.13}$$

Further analysis shows [8] that the second term in (2.12) is

$$\approx -\frac{Q_a^2 N_c}{\pi q^2}\left[\frac{2m_a^2 \ln(-q^2)}{q^2} + \ldots\right] \tag{2.14}$$

which is not only non-leading compared with (2.13), but of the same form as found by calculating Fig. 1 and retaining the effect of quark masses. Thus the masses appearing in the "chiral symmetry" formula (1.47) are in principle measurable in a high-energy current-induced reaction in QCD_2. (While the above analysis applied to q^2 large — but not real and positive which is the physical region — similar conclusions can be reached [7, 8] by averaging over the direct channel resonances.)

From this analysis we see how a parton model result which is clearly related (1.2) to the short-distance behaviour of the theory, and hence underwritten by asymptotic freedom, can be recovered [7, 8] in a model with quark confinement and is not altered by the long-distance properties of the theory.

2.3. Meson form factors [8]

We now turn to an application which is not underwritten by asymptotic freedom. In general a quark "form factor" has contributions both from a "bare" diagram (Fig. 16a)

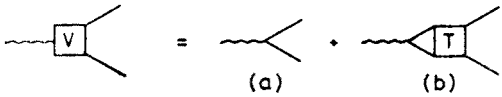

Fig. 16. Contributions to the quark form factor

and from a rescattering with a T matrix (Fig. 16b). Just as in the case of e^+e^- annihilation, Fig. 16 can be rewritten in the form

$$V(X) = 1 - \int_0^1 dY \frac{1}{(Y-X)^2} \int_0^1 dY' G(Y, Y'; q) \tag{2.15}$$

which can be written as

$$V(X) = \left(\frac{q^2}{m^2} - \frac{\gamma_a - 1}{X} - \frac{\gamma_b - 1}{1-X}\right) \int_0^1 dX' G(X, X'; q) \quad \text{for } 0 < X < 1, \tag{2.16}$$

by using the bound state equation (1.39). Unfortunately, diagrams cannot always be calculated "as if" the vertex V were just the "bare" one of Fig. 16a.

Consider a quasi-elastic meson form factor, for which the sum of leading order diagrams can be represented by Fig. 17a. The $-$ component of the part of the $(n \to m)$ transition form factor corresponding to the current hitting the a quark is

$$F^a_{-nm} = \frac{-2iQ_a}{\pi} \int d^2k \Gamma^{a\bar{b}}_n(k; p) S^a(k) V^a(k; q) S^a(k-q) \Gamma^{a\bar{b}}_m(k-q; p') S^b(k-p). \qquad (2.17)$$

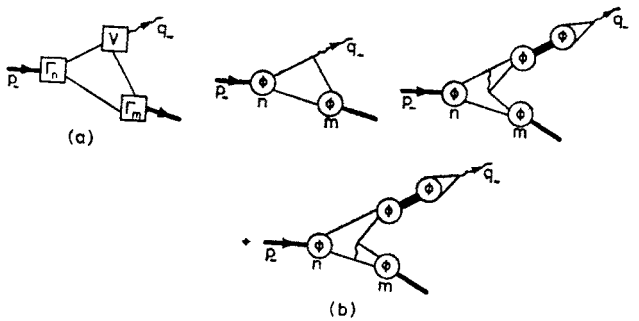

Fig. 17. (a) Feynman, and (b) x_-"time"-ordered perturbation theory d agrams for the meson form factor

When one does the k_+ integral in (2.17), one gets contributions corresponding to differential traditional x_- "time" ordered perturbation theory diagrams [8]. Each of these has energy denominators

$$\frac{1}{\left(\mu_n^2 - \frac{\gamma_a - 1}{X} - \frac{\gamma_b - 1}{1-X}\right)}$$

etc. which cancel against the numerator factors (2.3) and (2.16) in the meson-qq and current vertices. The resulting diagrams are shown in Fig. 17b: the first is the only time-ordered perturbation possibility when no T matrix is inserted, the latter are the two possible time-orderings with T matrices inserted. The resulting form factor (2.17) can be written as

$$F^a_{-nm} = 2Q_a p'_-(1-X) \left\{ \int_0^1 dZ \phi^{a\bar{b}}_m(Z) \phi^{a\bar{b}}_n(X + (1-X)Z) \right.$$

$$\left. + X^2 \int_0^1 dY \int_0^1 dZ \phi^{a\bar{b}}_m(Z) \frac{[\phi^{a\bar{b}}_n(XY) - \phi^{a\bar{b}}_n(X + (1-X)Z)]}{[X(1-Y) + (1-X)Z]^2} \int_0^1 dV G(Y, V; q) \right\}, \quad X \equiv q_-/p'_-,$$

corresponding in an obvious way to the diagrams of Fig. 16b. Note that in writing (2.18) we have explicitly extracted from some vertex functions a gluon which "turns" round

a quark so as to feed it into a wave function with momentum fraction between 0 and 1. The form of the diagrams of Fig. 16b and the formula (2.18) are particular examples of general features of calculations in QCD_2.

There is a general relation between q^2 and the variable X

$$m_m^2 = \frac{q^2}{X} + \frac{m_n^2}{1-X}. \tag{2.19}$$

When $X \to 0$, the second term in (2.18) disappears, leaving

$$F^a_{-nm} = 2Q_a p'_- \int_0^1 dZ \phi_n^{a\bar{b}}(Z)\phi_m^{a\bar{b}}(Z) = 2Q_a p'_- \delta_{nm}. \tag{2.20}$$

Thus only elastic form factors survive at $q^2 = 0$, they are correctly normalized and calculated by the "bare" current quark coupling.

Consider now the asymptotic behaviour of (2.18) in the limit $Q^2 = -q^2 \to \infty$. From (2.19) we see that

$$X \approx 1 - \frac{m_m^2}{Q^2} \to 1 \quad \text{as } Q^2 \to \infty, \tag{2.21}$$

so that (2.18) acquires a factor of $(Q^2)^{-1}$ from the external $(1-X)$ factor. In the first "bare" piece

$$\phi_m^{a\bar{b}}(X+(1-X)Z) \to \phi_m^{a\bar{b}}\left(1 - \frac{m_m^2}{Q^2}(1-Z)\right) = O\left(\left(\frac{m_m^2}{Q^2}\right)^{\beta_b}(1-Z)^{\beta_b}\right), \tag{2.22}$$

because of the vanishing property (1.40) of the meson wave functions. Thus the "bare" piece of the form factor has an over-all asymptotic behaviour of [8]

$$(Q^2)^{-1-\beta_b} \tag{2.23}$$

and a similar analysis of the second "rescattering" piece in (2.18) reveals the same asymptotic power law (2.23).

Several remarks should be made [8] about this result. First note that the form factor explicitly probes the $X \to 1$ behaviour of the meson wave function, just as expected by Feynman [25] and other parton advocates [28, 49]. On the other hand, at least in the reference frame used here, both "bare" and "rescattering" pieces are of the same order (2.23), and there is no direct description of the form factor in terms of a "bare" short-distance current-$q\bar{q}$ vertex [28], unlike the situation in e^+e^- annihilation where asymptotic freedom applied. If this feature carries over to QCD_4, it would make the absolute normalizations of large Q^2 form factors tricky to calculate and, when combined with the corresponding renormalization of "fixed angle" processes discussed in lecture 3, makes it difficult to relate [28] easily form factors to other "hard" processes. In this situation where asymptotic freedom is inapplicable, long-distance effects modify in an essential way. An obvious feature of (2.23) is that the simple integer power of the dimensional counting rules is not reproduced [8]. It is not clear whether this power renormalization is specific

to QCD_2: in QCD_4 the counting rules may be correct [50] even if the normalization of the graphs is more complicated. In any case $\beta_{u,d} \sim 0.02$ are small, and it is difficult to find a situation where β_s would be easy to observe.

2.4. Deep inelastic scattering [8]

The cross-section for $e+M \to e+X$ is determined by the absorptive part of the current correlation function indicated in Fig. 18a. This may be represented in terms of a structure function W:

$$W_{\mu\nu} = \left(p_\mu - \frac{\nu q_\mu}{q^2}\right)\left(p_\nu - \frac{\nu q_\nu}{q^2}\right)\frac{1}{m_n^2} W(q^2, \nu), \tag{2.24}$$

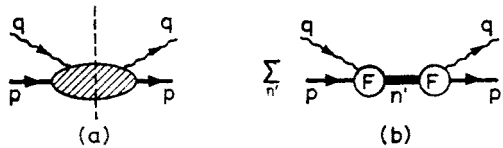

Fig. 18. (a) The absorptive part of the current correlation function, and (b) its representation as a sum of squares of meson form factors

where $\nu \equiv p_n \cdot q$. In leading order of $1/N_c$, the structure function is expressible [8] as a sum of squares of meson form factors (Fig. 18b):

$$W_{--} = (2\pi)^2 \sum_{n'} |F^a_{-n'n}(q^2) + F^{\bar{b}}_{-n'n}(q^2)|^2 \delta((p+q)^2 - m_{n'}^2), \tag{2.25}$$

where we include pieces where the current interacts with either the quark a or the antiquark $\bar{b}$ in the target meson. We will consider the Bjorken limit (1.3)

$$Q^2 = -q^2 \to \infty, \quad X_{Bj} \equiv \frac{Q^2}{2\nu} \text{ fixed.}$$

To get the inclusive cross-section we average over the high-mass resonances n', using (1.44) $\Delta m^2_\infty = \pi^2 m^2$ and

$$n' \approx \frac{2\nu}{\pi^2}(1 - X_{Bj}). \tag{2.26}$$

Taking the "bare" piece of (2.18), we can use the scaling relation (1.46) to get

$$F^a_{-nn'}(\text{bare}) \underset{Bj}{\approx} \frac{2Q_a p_- X_{Bj}}{Q^2} \phi_n^{a\bar{b}}(X_{Bj}) \int_0^\infty d\xi \phi^a(\xi) \underset{Bj}{\approx} p_- \frac{\pi}{\sqrt{2}} \frac{Q_a m_a}{Q^2} X_{Bj} \phi_n^{a\bar{b}}(X_{Bj}), \tag{2.27}$$

where we have used an identity [8] for the scaling function (1.46) which ensures the asymptotic freedom result (2.13) for the average over direct channel resonances in $e^+e^- \to$ hadrons. A little bit of analysis [8] shows that the "rescattering" term in (2.18) is $O(\ln Q^2/Q^4)$

in the Bjorken limit, and so may be discarded. The antiquark form factor in (2.25) has a Bjorken limit

$$F^{\bar{b}}_{-nn'} \underset{\mathrm{Bj}}{\approx} (-1)^{n'} p_- \frac{\pi}{\sqrt{2}} \frac{Q_b m_b}{Q^2} X_{\mathrm{Bj}} \phi_n^{a\bar{b}}(1 - X_{\mathrm{Bj}}). \tag{2.28}$$

In combining the two results (2.27) and (2.28) in the expression (2.25) for W_{--}, interference terms could in principle arise, but detailed analysis confirms the intuitive expectation that they may be neglected in the Bjorken limit. We conclude that

$$\lim_{\mathrm{Bj}} \nu^2 W(q^2, \nu) = 2\pi^2 \{Q_a^2 m_a^2 [\phi_n^{a\bar{b}}(X_{\mathrm{Bj}})]^2 + Q_b^2 m_b^2 [\phi_n^{a\bar{b}}(1 - X_{\mathrm{Bj}})]^2\} \tag{2.29}$$

which is the same as one would have got from the simple "handbag" diagram (Fig. 2) of the naive quark-parton model [25, 49]. (The mass factors in (2.29) arise because of the kinematics of the vector coupling in 2 dimensions: they are completely canonical.)

Once again, a parton result underwritten by asymptotic freedom is recovered in QCD_2 despite the long-range effects of confinement. The interpretation that deep inelastic scattering probes the meson wave function is borne out. The Drell-Yan-West [51] threshold relation holds between the threshold behaviour as $X_{\mathrm{Bj}} \to 1$ of the structure function and the power behaviour (2.23) of the quasi-elastic form factors. The behaviour as $X_{\mathrm{Bj}} \to 0$ of the structure function (2.29) is related to the Regge behaviour of total cross-sections discussed in Lecture 3, in just the way suggested by Abarbanel, Goldberger and Treiman [52] . One question which has not been resolved in QCD_2 is to what extent the approach to the Bjorken scaling limit is governed by quark and hadron target masses in the manner advocated by Georgi and Politzer [53]. It would be interesting to study this question in QCD_2.

2.5. Lepton pair production in hadron collisions [11]

It was suggested by Drell and Yan [26] that this reaction might be described by the simple parton-antiparton annihilation model described in Fig. 4. Unfortunately, short-distance asymptotic freedom ideas have not been shown [54] to apply to this process. This makes lepton pair production interesting to study in QCD_2, being a borderline situation where we may hope to acquire some new insight. The possibilities to be confronted are that other (bremsstrahlung?) diagrams may not be negligible in the scaling limit [55], and that the annihilation diagram may be modified. This could either be via final state spectator quark-antiquark recombination into mesons [56], or by the annihilating quark-antiquark scattering through bound states before creating the time-like photon which yields the lepton pair [57].

These questions have been studied in $O(1/N_c)$ for QCD_2 by Kripfganz and Schmidt [11], we refer to their paper for details and just quote their conclusions here. They showed that bremsstrahlung diagrams were suppressed by $O(s^{-4})$ relative to the annihilation diagrams, the suppression arising because at least two gluon propagators have to carry large momenta $k_-^2 = O(s)$. Resonances in the time-like Q^2 l^+l^- channel were found not to contribute in the scaling limit. This cancellation arose from the same mechanism as

that which removes the Pomeron [10, 12, 13], as discussed in Lecture 3. The remaining diagrams have exactly the Drell-Yan [26] parton-antiparton annihilation form, and numerical analysis showed that the normalization was exactly that expected for the naïve Drell-Yan graph, unaltered by final state interaction effects [56].

Although it is very interesting that QCD_2 reproduces a parton model result which is not underwritten by asymptotic freedom, the significance for QCD_4 of this result is not clear. For one thing, other fundamental sub-diagrams besides the simple $q\bar{q} \to \gamma^* \to l^+l^-$ will scale, and perhaps contribute to the large Q^2 lepton pair spectrum [55]. For another thing, the Pomeron cancellation of Lecture 3 presumably does not occur in QCD_4, so that resonant contributions in the virtual photon channel may not be negligible. Finally, electroproduction scaling is not exact in QCD_4, and the Drell-Yan scaling must surely also be violated. It has been suggested [58] that scaling violations in Drell-Yan may take the form of convoluting in (1.7) the effective Q^2 dependent quark distributions which are determined by asymptotic freedom calculations for electroproduction.

2.6. $e^+e^- \to M+X$ [9]

According to the parton model [25, 49], the inclusive cross-section in e^+e^- annihilation should have a simple description (Fig. 3) in terms of quark-partons fragmenting into final-state hadrons. This hadronization process presumably involves long-distance confinement phenomena in an essential way. It is easy to show that in the limit

$$Q^2 \to \infty : X_F \equiv \frac{2p^{c.m.}}{Q} \text{ fixed}, \tag{2.30}$$

the cross-section is related to a light-cone singularity [48]. On the other hand, this is just one singularity of a complicated four field Green's function, and one may expect it to be renormalized by long-distance effects. That this happens can be understood by considering unitarity [9].

The naïve parton diagram for $e^+e^- \to X$ is $O(N_c)$, whereas the naïve diagrams for electroproduction $e+M \to e+X$ and inclusive annihilation $e^+e^- \to M+X$ are both $O(N_c^0)$. Since by unitarity

$$\sigma(e^+e^- \to X) = \sum_m \int_0^1 dX_F X_F \frac{d\sigma}{dX_F}(e^+e^- \to M+X) \tag{2.31}$$

a contradiction seems to arise. This was pointed out by Einhorn [9], who also gave a resolution [35, 36]. Included in Fig. 19a are diagrams with direct channel resonances as shown

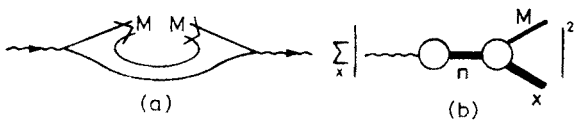

Fig. 19. (a) Contribution to $e^+e^- \to M+X$ which is formally $O(N_c^0)$, and (b) a direct channel resonance piece

in Fig. 19b. Since the three-meson vertex is $O(1/\sqrt{N_c})$ and $\Gamma(n \to M+X) = O(1/N_c)$ [34, 35], the inclusive cross-section exhibits oscillations which become sharper and sharper as $N_c \to \infty$, as indicated in Fig. 20. These must be averaged in order to give a sensible inclusive hadron cross-section. We have from Fig. 19b

$$\sigma(e^+e^- \to M+X) \propto \left| \sum_n \sum_X \frac{\gamma_n G_{nMX}}{(q^2 - m_n^2) + i\Gamma_n m_n} \right|^2 \tag{2.32}$$

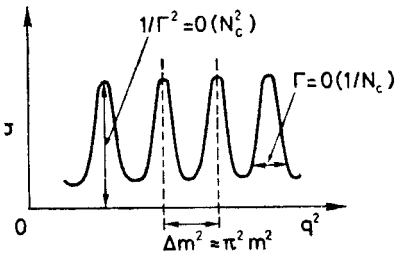

Fig. 20. Oscillations due to narrow resonances in $\sigma(e^+e^- \to \text{hadrons})$

and since the resonances do not interfere in the large N_c limit

$$\sigma(e^+e^- \to M+X) \sim \sum_n \gamma_n^2 \frac{1}{(q^2 - m_n^2)^2 + m_n^2 \Gamma_n^2} \sum_X G_{nMX}^2. \tag{2.33}$$

Averaging over the asymptotic resonance separation

$$\Delta m_\infty^2 = \left(\frac{g^2 N_c}{\pi}\right) \pi^2$$

we find

$$\sigma(e^+e^- \to M+X) \sim \gamma_n^2 \frac{1}{\Gamma_n} \left(\sum_X G_{nMX}^2 \right). \tag{2.34}$$

To get $\sigma(e^+e^- \to X) = O(N_c)$, γ_n^2 must be $O(N_c)$ as $N_c \to \infty$. But then Γ_n and $\sum_X G_{nMX}^2$ are clearly both $O(1/N_c)$, so that Eq. (2.34) implies

$$\sigma(e^+e^- \to M+X) = O(N_c), \tag{2.35}$$

as required by the unitarity equation (2.31). This paradox [9] and its resolution [9] entail a breakdown of naïve parton models [49] in which interactions between the $q\bar{q}$ pair are neglected entirely. However, they do not conflict with Feynman's [25] parton fragmentation description, at least in QCD_2.

Some relevant "time"-ordered perturbation theory diagrams to calculate for G_{MXn} are shown in Figs 21(b), (c): note the role the gluons play in "turning" quarks. We will discuss

G_{MXn} in more detail in Lecture 3. Suffice it for now to say that in the limit (2.30):

$$m_n^2 \to \infty, \quad m_X^2/m_n^2 \approx (1-X_F) \text{ finite}, \tag{2.36}$$

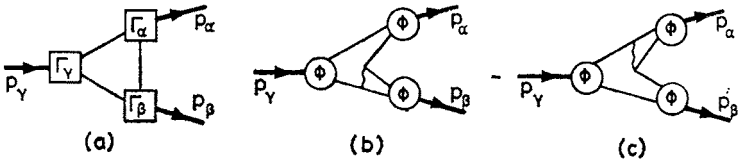

Fig. 21. (a) Feynman, and (b), (c) x-"time"-ordered perturbation theory diagrams for the 3 meson vertex

the diagram in Fig. 21(b) drops away, and we are just left with Fig. 21(c) which gives

$$\frac{1}{\sigma} X_F \frac{d\sigma}{dX_F} \approx \sum_a D_{a\to M}(X_F) \tag{2.37}$$

where

$$D_{a\to M}(X_F \equiv \frac{1}{D_a} \lim_{\substack{n,n_X\to\infty \\ n_X/n = 1-X_F}} \left[\frac{1-X_F}{X_F} \int_0^1 dX \int_0^1 dY \frac{\phi_M^{b\bar{a}}(X)\phi_{n_X}^{c\bar{b}}(Y)\phi_n^{c\bar{a}}((1-X_F)Y)}{\left(X + \frac{(1-X_F)}{X_F}(1-Y)\right)^2} \right]^2 \tag{2.38a}$$

with

$$D_a \equiv \sum_b \int_0^1 dX_F \lim_{\substack{n,n_X\to\infty \\ n_X/n = 1-X_F}} \left[\frac{1-X_F}{X_F} \int_0^1 dX \int_0^1 dY \frac{\phi_M^{b\bar{a}}(X)\phi_{n_X}^{c\bar{b}}(Y)\phi_n^{c\bar{a}}((1-X_F)Y)}{\left(X + \frac{(1-X_F)}{X_F}(1-Y)\right)^2} \right]^2 \tag{2.38b}$$

Equations (2.37) and (2.38) yield a parton fragmentation picture for the hadronic final state.

Similar arguments apply to some contributions to the final state in electroproduction $e+M \to e+M'+X$, and we conclude that QCD_2 probably has the desired universality of final states in time-like and space-like Q^2 processes. In Lecture 3 we will see that this universality may even extend [12] to hadron-hadron collisions.

3. Hadron-hadron collisions

3.1. Preliminaries: the three-meson vertex

In this final lecture we will study various aspects of purely hadronic reactions in QCD_2. Among the topics to be discussed [10, 12, 13] are Regge behaviour, duality between direct and crossed channels, a possible analogue to fixed angle scattering, the existence of the Pomeron, and inclusive hadronic reactions. The phenomenological ideas we want to test were set out in Section 1.2: we also hope to find some novel properties which might be relevant to QCD_4.

Just as the quasi-elastic form factor (2.18) was a crucial ingredient in building up the deep inelastic structure functions, so the three-meson vertex G_{123} will be an essential building block in constructing hadronic scattering amplitudes. To obtain G_{123} we must calculate the diagram of Fig. 21a. This can be written as a Feynman integral [12]

$$iG_{123} = N_c\left(-2i\sqrt{\frac{\pi}{N_c}}\right)^2\int\frac{d^2k}{(2\pi)^2}$$

$$\times\frac{(-1)^{n_2+n_3}/p_{1-}\Gamma_1^{b\bar{a}}\left(\frac{k_-}{p_{1-}}\right)\frac{1}{p_{2-}}\Gamma_2^{b\bar{c}}\left(\frac{-k_-}{p_{2-}}\right)\frac{1}{p_{3-}}\Gamma_3^{a\bar{c}}\left(\frac{p_{1-}-k_-}{p_{3-}}\right)\left(\frac{i}{2}\right)^3}{\left[k_+-\frac{\tilde{m}_b^2+i\varepsilon}{2k_-}\right]\left[(p_1-k)_+-\frac{\tilde{m}_a^2+i\varepsilon}{2(p_1-k)_-}\right]\left[(p_2+k)_+-\frac{\tilde{m}_c^2+i\varepsilon}{2(p_2+k)_-}\right]}. \tag{3.1}$$

As in the analysis of the form factor (2.17), we proceed by performing the k_+ integral in (3.1), which gives us two x_- "time"-ordered perturbation theory diagrams of Figs 21(b), (c). They can be written in the form

$$G_{123} = \sqrt{\frac{\pi}{N_c}}\,2m^2\,\frac{p_{1-}}{p_{2-}}\int_0^1 dX\int_0^1 dX'\,\frac{(-1)^{n_2}\phi_1^{b\bar{a}}(X)\phi_2^{b\bar{c}}(X')}{\left(X\dfrac{p_{1-}}{p_{2-}}+X'\right)^2}$$

$$\times\left[\phi_3^{c\bar{a}}\left(\frac{1-X'}{1+p_{1-}/p_{2-}}\right)-\phi_3^{c\bar{a}}\left(\frac{1+X\dfrac{p_{1-}}{p_{2-}}}{1+p_{1-}/p_{2-}}\right)\right]. \tag{3.2}$$

Notice that the vertex (3.2) can be written down very simply in terms of [8, 10, 12, 13]
— meson wave functions $\phi_n^{a\bar{b}}(k_-/p_{n-})$
— quark propagators 1
— gluon propagators $1/k_-^2$
The energy denominators from the quark propagators in (3.1) cancel with the numerators (2.3), just as in the analysis of e^+e^- annihilation in Section 2.2: again no real quarks! The gluon propagators in (3.2) play the rôle of "turning" the quarks so that they fall in the "acceptance" $0 \leqslant X \leqslant 1$ of the meson wave functions. Note the factor $1/\sqrt{N_c}$ outside the integral in (3.2), and also the relative−sign in the integrand. The latter reflects the relative−sign between the colours of the quark and antiquark which is felt when the gluon is "flipped" from one to another as in Figs 21(b), (c).

It is kinematically convenient to work in the rest frame of the particle 3 so that

$$m_3 = \sqrt{s} = \sqrt{(p_1+p_2)^2}.$$

Then we may define 1 to be a left-moving particle so that its light-like momentum

$$p_{1-} \equiv \frac{1}{\sqrt{2}}(p_0-p_1) \underset{s\to\infty}{\approx} \sqrt{s} \tag{3.3a}$$

is much larger than that for the right-moving particle 2:

$$p_{1-} \gg p_{2-} : p_{2-} \equiv \frac{1}{\sqrt{2}}(p_0 - p_1)_2 \underset{s\to\infty}{\approx} \frac{m_2^2}{\sqrt{s}} . \tag{3.3b}$$

These limits will be useful when we discuss the high energy behaviour of scattering amplitudes.

3.2. Forward meson-meson scattering

As discussed in Section 1.3, the leading $O(1/N_c)$ diagrams for meson-meson scattering are those shown in Fig. 8(e) [32, 38]. In the limit $s \to \infty$, t fixed the combination $A_{st} + A_{tu}$ should give Regge behaviour. The third diagram A_{us} should $\to 0$ relative to the other two:

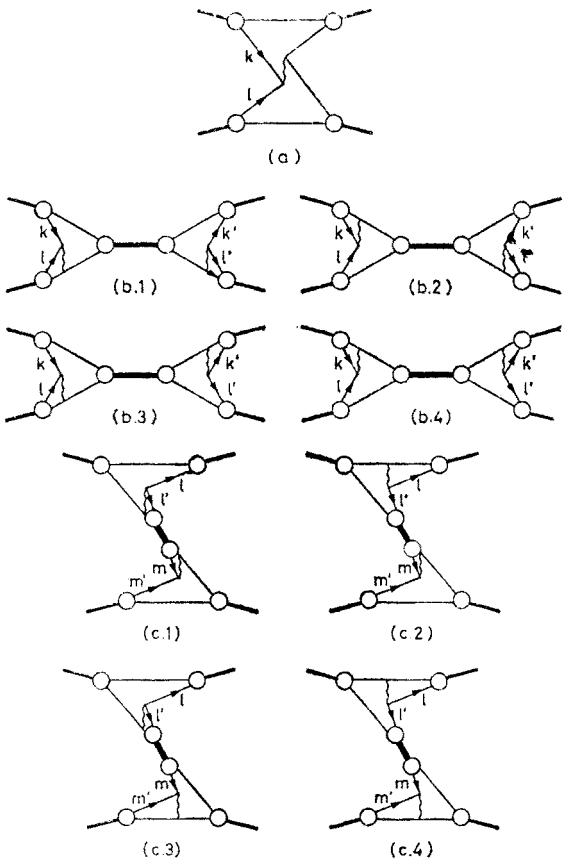

Fig. 22. "Time"-ordered perturbation theory diagrams for A_{st}

it has no crossed channel singularities at finite momentum transfer, as it depends only on the variables $s(\to \infty)$ and $u(\to -\infty)$. The x_- "time"-ordered perturbation theory diagrams for A_{st} are shown in Fig. 22. Rather than calculate explicitly the high energy behav-

iour of each diagram, let us just look at

$$\text{Im } A_{st} = \sum_n G_{12n}\pi\delta(s-m_n^2)G_{1'2'n} \tag{3.4}$$

and estimate the high energy behaviour of G_{12n} (3.2).

We see from (3.3) that in the Regge limit $p_{1-}/p_{2-} \approx s/m_2^2$, so that in order to keep small the gluon propagator

$$\frac{1}{(Xp_{1-}/p_{2-}+X')^2}$$

in (3.2), we should keep X small. Introducing η:

$$X \equiv \eta\frac{p_{2-}}{p_{1-}} \approx \eta\frac{m_2^2}{s}, \tag{3.5}$$

we find $p_{1-}/p_{2-}\,dX = d\eta = O(1)$ in Eq. (3.2), as well as the gluon propagator $1/(\eta+X') = O(1)$, and inserting the scaling version (1.46) of the meson wave function $\phi_3^{c\bar{a}}$ we find

$$G_{123} \underset{s\to\infty}{\approx} 2\sqrt{\frac{\pi}{N_c}}(-1)^{n_2}m^2\int_0^\infty d\eta\int_0^1 dX'\,\frac{\phi_1^{b\bar{a}}\left(\eta\dfrac{m_2^2}{m_3^2}\right)\phi_2^{b\bar{c}}(X')}{(\eta+X')^2}$$

$$\times\left[\phi^c\left((1-X')\frac{m_2^2}{m^2}\right)-\phi^c\left((1+\eta)\frac{m_2^2}{m^2}\right)\right]. \tag{3.6}$$

Now comes the crunch: from the vanishing (1.40) of the meson wave function at its kinematic boundary:

$$\phi_1^{b\bar{a}}\left(\eta\frac{m_2^2}{m_3^2}\right) \underset{s\to\infty}{\approx} C_1^{b\bar{a}}\eta^{\beta_b}\left(\frac{m_2^2}{s}\right)^{\beta_b}, \tag{3.7}$$

so that $G_{123} = O(s^{-\beta_b})$ as $s\to\infty$ [59]. A somewhat more detailed analysis [12] shows that

$$G_{123} \underset{s\to\infty}{\approx} 2\sqrt{\frac{\pi}{N_c}}m^2\left(\frac{s}{m^2}\right)^{-\beta_b}V_1^{b\bar{a}}V_2^{b\bar{c}}, \tag{3.8a}$$

where

$$V_1^{b\bar{a}} = C_1^{b\bar{a}}\sqrt{\frac{\pi\sin\pi\beta_b}{C_b}}, \text{ etc.} \tag{3.8b}$$

To get the absorptive part of the amplitude for $1+2\to 1'+2'$ we just use (3.4) and average over the asymptotic spacing $\Delta m_\infty^2 = m^2\pi^2$ of direct channel resonances

$$\text{Im } A_{st} \underset{s\to\infty}{\approx} \frac{4}{N_c}m^2\left(\frac{s}{m^2}\right)^{-\beta_b-\beta_d}(V_1^{b\bar{a}}V_{1'}^{d\bar{a}})(V_2^{b\bar{c}}V_{2'}^{d\bar{c}}) \tag{3.9}$$

and similar power behaviour can be demonstrated for Re A_{st} and for A_{tu}. The result (3.9) we [10] would like to interpret as embryonic "Regge" behaviour: why?

First notice that the asymptotic power of s

$$\alpha_{b\bar{d}}(0) \equiv -\beta_b - \beta_d \tag{3.10}$$

is non-integer, unlike a normal fixed pole [60]. Furthermore, it depends through (1.41) on the quark quantum numbers $(b, \bar{d})$ exchanged in the crossed channel. Also, this power is independent of the specific external bound state mesons. As indicated by the parentheses in (3.9), Im A_{st} factorizes in the crossed channel, as expected of a Regge pole. Going beyond the scope of these lectures, it has also been shown [12] that 2–3, 2–4 and 3–3 meson amplitudes exhibit the multi-"Regge" power behaviour expected on the basis of (3.9).

If you accept the "Regge" interpretation of (3.9), then there are several amusing remarks to be made. First, notice how Feynman's [25] interpretation of Regge behaviour as reflecting the exchange of wee quarks is explicitly realized in this model, where the small X part of the meson wave function (3.7) is being probed. Notice also that because Im $A_{st} \to 0$ as $s \to \infty$ (also Re A_{st}, A_{tu}, $A_{us} \to 0$ can be checked explicitly) the 2–2 forward elastic amplitudes satisfy unsubtracted dispersion relations (assuming they are analytic, which we have no proof of, but have no reason to doubt). Therefore the dual [30, 38] property (1.9) of Fig. 5:

$$\sum \text{direct channel resonances} = \sum \text{crossed channel Regge poles},$$

clearly holds in QCD_2. Furthermore, since there are no exotic states in this order, the different Regge trajectories $(\varrho, f, \omega, A_2)$ will be strongly exchange degenerate [32] in $O(1/N_c)$.

As a confirmation of the "Regge" interpretation of the asymptotic form (3.9), we should mention that a connection can be made [12] with the lowest mass crossed channel meson pole in the limit of small quark mass. First recall equation (1.41)

$$\pi\beta_a \cot \pi\beta_a + \left(\frac{m_a}{m}\right)^2 - 1 = 0.$$

Then as was mentioned earlier

$$m_a \to \infty \Rightarrow \beta_a \to 1, \tag{3.11a}$$

while

$$m_a \to 0 \Rightarrow \beta_a \approx \left(\frac{\sqrt{3}}{\pi m}\right) m_a \to 0. \tag{3.11b}$$

Combining with the formula (3.10) for the Regge "intercept", we see that for small quark masses $m_a, m_b \to 0$:

$$\alpha_{a\bar{b}}(0) \approx -\frac{\sqrt{3}}{\pi m}(m_a + m_b). \tag{3.12}$$

But as noted in Section 1.6

$$(m_0^{a\bar{b}})^2 \approx \frac{\pi m}{\sqrt{3}}(m_a + m_b) \tag{3.13}$$

as m_a, $m_b \to 0$. Thus the Regge "intercept" and the bound state pole position come together as m_a, $m_b \to 0$. We can imagine drawing an embryonic Chew-Frautschi plot as in Fig. 23, with a line interpolating between (3.12) and (3.13) which has slope

$$\alpha_0' \approx \frac{3}{\pi^2 m^2} = \frac{3}{\pi g^2 N_c} . \tag{3.14}$$

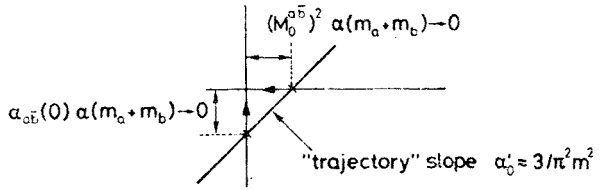

Fig. 23. Embryonic Chew-Frautschi plot, showing the limits of "Regge" intercept and lowest bound state mass as quark masses $\to 0$

It is this "slope" which, when given the real world value of 0.9 GeV^{-2} and used together with m_π^2 and $m_{K'}^2$, gave $m_{u,d} = O(10)$ MeV, $m_s = O(200)$ MeV in Lecture 1, corresponding to $\beta_{u,d} \approx 0.01$, $\beta_s \approx 0.21$, $\beta_c \sim 0.9$. The correspondence (3.12) and (3.13) between Regge and crossed channel poles goes deeper: the decoupling of the zero-mass meson can also be seen as the appropriate zero in the Regge residue as $\alpha^{a\bar{b}}(0) \to 0$.

Before leaving the "Regge" behaviour (3.9) we should note some intriguing features which one is tempted [12] to generalize to QCD_4.

— Intercepts are additive in the quarks exchanged in the crossed channel. Although the absolute values of the intercepts (3.10) are unrealistic (4-dimensional spin effects?) the differences are quite reasonable: we find

$$\alpha_\varrho(0) - \alpha_{K^*}(0) = \beta_s - \beta_d = \alpha_{K^*}(0) - \alpha_\phi(0) \approx 0.2 \tag{3.15}$$

which relations are not inconsistent with experiment.

— There is an absolute lower limit to Regge intercepts, because of (3.10) and (3.11a). Other people [61] have conjectured that 4-dimensional Regge trajectories may be bounded below as $t \to -\infty$, and Regge slopes are apparently positive, so perhaps a similar limit applies to Regge intercepts in 4 dimensions [62]. Using the natural hypothesis

$$\alpha_{q\bar{q}'}(0) = \alpha_\varrho(0) + \beta_u + \beta_d - \beta_q - \beta_{q'},$$

one is led to

$$\alpha_{q\bar{q}'}(0) \geqslant \alpha_\varrho(0) - 2 \approx -1\tfrac{1}{2} . \tag{3.16}$$

In particular, one might suspect

$$\alpha_{c\bar{c}}(0) \approx -1\tfrac{1}{2} , \quad \alpha_{D^*}(0) \approx -\tfrac{1}{2} . \tag{3.17}$$

The relatively high intercepts (3.17) may be good news for people looking for charm in quasi two-body reactions.

— Direct channel factorization of the amplitude is a feature not only of the Regge limit (3.9) but also more generally for $s > 0$. This results from having just one direct channel resonance at each mass. We know [63] of no evidence against direct channel factorization of amplitudes in 4 dimensions [64], and it may be an amusing property to look for.

There is a connection between form factor and Regge powers implicit in Eqs (2.23) and (3.9). It is not clear this relation should be abstracted for 4 dimensions. As emphasized during their derivations, the form factor result (2.23) comes from probing the $X \to 1$ part of the meson wave function, whereas the Regge result (3.10) came from the $X \to 0$ part of the wave function [50]. It is only in the valence $q\bar{q}$ model of the meson wave function enforced by QCD_2 in the $1/N_c$ expansion that there is a direct connection between $X \to 0$ and $X \to 1$. We may note in passing that the relation (2.33, 3.10) between form factor and Regge powers is not that advocated by Bjorken and Kogut [65] on the basis of their correspondence principle.

3.3. A possible analogue for fixed angle scattering

Strictly speaking, our interpretation of (3.9) as indicating embryonic Regge behaviour in QCD_2 is as yet incomplete. While Re A_{st} and A_{tu} can be shown to have the same power behaviour (3.10), what of A_{us}? This subamplitude should be asymptotically negligible as $s \to \infty$, t fixed, $u \to -\infty$. Since both arguments of A_{us} become infinite in this Regge limit, it may well be that for A_{us} it is the analogue of a fixed angle limit ($\theta = \pi$). In 4 dimensions, all of $s, t, u \to \infty$ in the fixed angle limit, but only 2 of them appear in any individual $O(1/N_c)$ subamplitude A_{st}, A_{tu} or A_{us}.

The limit of A_{us} that we seek can be estimated from Fig. 22 by considering the case

$$p'_{1-} = O\left(\frac{1}{\sqrt{s}}\right), \quad p'_{2-} = O(\sqrt{s}).$$

Look at Fig. 22a for example: the large incoming p_{1-} must be routed across the diagram via the gluon, which necessarily has momentum $O(s)$, so that the propagator contributes a factor $O(1/s)$ to the integral

$$A_{(a)} = 4g^2 \int_0^{p_{1'-}} dk_- \int_0^{p_{2-}} dk'_- \phi_1^{a\bar{b}}\left(\frac{k_-}{p_{1-}}\right) \phi_2^{b\bar{c}}\left(\frac{p_{2-}-k'_-}{p_{2-}}\right)$$

$$\times \frac{\phi_{2'}^{d\bar{c}}\left(\frac{p_{2'-}-k'_-}{p_{2'-}}\right) \phi_{1'}^{a\bar{d}}\left(\frac{k_-}{p_{1'-}}\right)}{(p_{1-}+p_{2-}-k_--k'_-)^2}. \tag{3.18}$$

The k_- and k'_- integration regions in (3.18) are clearly both $O(1/\sqrt{s})$. Also, the large momentum transfer across the diagram forces the $\bar{b}$ quark emerging from meson 1 to carry essentially all its momentum: this induces a wave function boundary suppression $O(s^{-\beta_a})$. Similarly there is a factor $O(s^{-\beta_c})$ from the vanishing of $\phi_2^{\bar{c}c}$. Over-all then, Fig. 22a behaves as [10, 12]

$$s^{-2-\beta_a-\beta_c} \tag{3.19}$$

in this limit. In the other diagrams of Fig. 22, there are different possible routings of the large momentum across the diagram, all of which have the s^{-2} factor in (3.19), but with all possible wave function suppression factors:

$$s^{-2-\beta_a-\beta_b}, \quad s^{-2-\beta_a-\beta_c}, \quad s^{-2-\beta_a-\beta_d}, \quad s^{-2-\beta_b-\beta_c},$$

$$s^{-2-\beta_b-\beta_d} \quad \text{and} \quad s^{-2-\beta_c-\beta_d}. \tag{3.20}$$

The result (3.20) indicates that $|A_{us}| \ll |A_{st}|, |A_{tu}|$ in the "Regge" limit $s \to \infty$, t fixed, as we wanted. As far as the fixed angle interpretation of (3.20) is concerned, the renormalization powers $s^{-\beta}$ may be an artefact [50] of QCD_2, as was suggested in the discussion of form factors in Section 2.3. In any case, $\beta_{u,d}$ are very small and no-one has thought of a realistic case where none of the different combinations in (3.20) would involve u or d quarks. Notice that because all the diagrams in Fig. 22 contribute, with a motley collection (3.20) of powers, the fixed angle cross-section cannot be written as a simple product of form factors [66], and the relative normalization of form factors and fixed angle behaviour is non-trivial [28]. Like the form factor [8], fixed angle scattering in QCD_2 is not a pure short distance process, but is essentially renormalized by long distance effects.

3.4. The Pomeron?

As mentioned in Section 1.2, the $O(1/N_c^2)$ diagram shown in Fig. 8d is expected [31, 35, 36] to yield the bare Pomeron singularity. This happens in the dual resonance model [38], and phenomenological models based on the same diagrams have been proposed in the context of QCD [67]. In the dual model, the Pomeron can be thought of as the exchange of a cylinder or closed string (Fig. 9b). In QCD, one expects the exchange to feature "polyeikonalized" gluons (Fig. 9c), and the spin 1 of the gluons then suggests that $\alpha_P \approx 1$ in some approximation. In the dual model the cylinder is a more or less normal Regge trajectory, with particle poles. Such "Pomeronium" particles are also expected in QCD_4, because gluons are expected to form bound states ("gluonium") just as quarks form $q\bar{q}$, etc., bound states. (Consider a world with gluons but no quarks: presumably colour is confined in the same way as in the real world, because the infrared properties of theory are independent of the existence of massive particles. If such a theory is non-trivial, its states can only be gluonia: detecting their analogues in the real world is a different kettle of fish [39].) Dual and QCD_4 models suggest that $\alpha'_P \approx O(\frac{1}{2})\ \alpha'_R$ [68], so that the Pomeron trajectory should pass $J = 2$ when $t = 0(+2)\ \text{GeV}^2$. Mixing between the f, f' and Pomeron trajectories would be very complicated in this region, but presumably dual models or QCD_4 would predict three $I = 0$, $C = +1$ trajectories and three $J = 2$ states. On the other hand, in a more general dual framework, the bare Pomeron may be regarded as the shadow of non-resonant two cluster production. There is no obvious reason why the Pomeron would have crossed channel particle poles [69], or why the Pomeron intercept should necessarily be 1. Indeed, Chew and Rosenzweig [69] and others identify the Pomeron and f, so that they only have two $I = 0$, $C = +1$ trajectories. The two clusters may be regarded as coming from cutting along two generators of the dual cylinder.

To study the nature of the Pomeron in QCD_2, we study [10, 12, 13] the imaginary part of Fig. 8(f), which has the structure indicated in Fig. 9(a):

$$\text{Im } A = \frac{1}{4\pi^2}\int \frac{dM_1^2 dM_2^2}{\lambda^{1/2}(s, M_1^2, M_2^2)} |A_{tu}(s, M_1^2, M_2^2)|^2, \tag{3.21}$$

where λ is the usual phase space function. The general expectation is that the integration regions where M_1^2 and M_2^2 are both finite would give something like a Regge-Regge cut, but subject to the usual Mandelstam cancellation, whereas the region

$$M_1^2 M_2^2 = O(m^2 s) \tag{3.22}$$

should give Regge pole renormalization and break exchange degeneracy. The region

$$M_1^2 = O(s), \quad M_2^2 = O(s) \tag{3.23}$$

should give a new Pomeron singularity according to the dual model/QCD_4 ideology discussed earlier. In the limit (3.23) the phase space integral

$$\int \frac{dM_1^2 dM_2^2}{\lambda^{1/2}} = O(s) \tag{3.24}$$

and if we work in the centre-of-mass frame:

$$p_{1-} \approx \sqrt{s}, \quad p_{2-} \approx \frac{m_2^2}{\sqrt{s}},$$

it happens that

$$\frac{p_{1'-}}{p_{1-}} = O(1), \quad \frac{p_{2'-}}{p_{1-}} = O(1). \tag{3.25}$$

Hence both the quark and the antiquark from meson 1 must carry a finite fraction of its momentum. One might therefore naïvely expect $|A_{tu}| = O(1)$, as there would be no suppressions analogous to (3.10) coming from pushing quarks close to $X = 0$ or 1. Equations (3.21) and (3.24) would then yield Im $A = O(s)$, and a Pomeron with $J = 1$.

There are 11 diagrams contributing [10] to A_{tu} in x_- "time"-ordered perturbation theory, which are shown in Fig 24. Let us consider as an example the diagrams 24(d). Using the graph rules alluded to earlier, and developed in more detail in Refs [8, 12], their sum can be written as

$$A_{tu(d)} = -\frac{4\pi m^2}{N_c}\sum_n \left\{\left(\frac{p_{1'-}}{p_{1-}-p_{1'-}}\right)\int_0^1 dX \int_0^1 dX' \frac{\phi_1^{d\bar{a}}(X)\phi_n^{d\bar{b}}(X')}{\left(X\dfrac{p_{1'-}}{p_{1'-}-p_{1'-}}+X'\right)^2}\right.$$

$$\left.\times\left[\phi_1^{b\bar{a}}\left(\frac{(p_{1-}-p_{1'-})(1-X')}{p_{1-}}\right)-\phi_1^{b\bar{a}}\left(\frac{(p_{1-}-p_{1'-})+p_{1'-}X}{p_{1-}}\right)\right]\right\}$$

$$\times \frac{1}{t-m_n^2}\left\{\left(\frac{p_{1-}-p_{1'-}}{p_{2-}}\right)\int_0^1 dY \int_0^1 dY' \frac{\phi_2^{d\bar{c}}(Y')\phi_n^{d\bar{b}}(Y)}{\left(Y\dfrac{p_{1-}-p_{1'-}}{p_{2-}}+Y'\right)^2}\right.$$

$$\left.\times\left[\phi_{2'}^{c\bar{b}}\left(\frac{p_{2-}(1-Y')}{p_{2'-}}\right)-\phi_{2'}^{c\bar{b}}\left(\frac{p_{2-}+(p_{1-}-p_{1'-})}{p_{2'-}}\right)\right]\right\}. \tag{3.26}$$

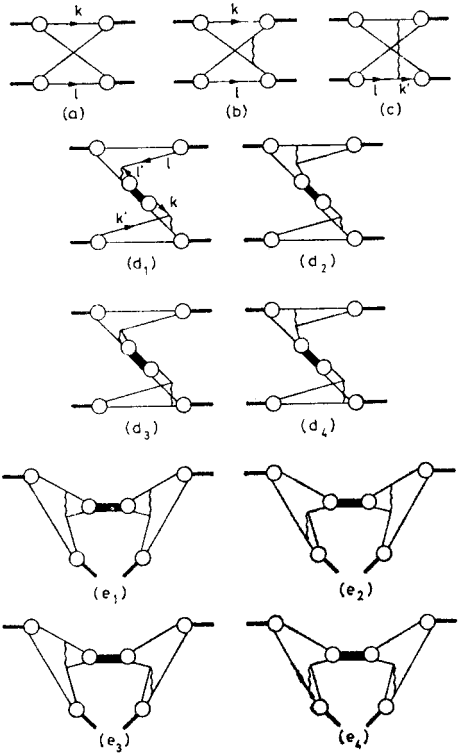

Fig. 24. "Time"-ordered perturbation theory diagrams for A_{tu}

The integral over each individual product of six wave functions ϕ in (3.26), each corresponding to an individual diagram of Fig. 24(d), is $O(s^0)$ but there is a cancellation. The leading behaviour comes when the gluon propagators are "soft":

$$X' = O\left(\frac{m^2}{s}\right), \quad X = O\left(\frac{m^2}{s}\right) \tag{3.27}$$

In this case

$$\left[\phi_1^{b\bar{a}}\left(\frac{(p_{1-}-p_{1'-})(1-X')}{p_{1-}}\right)-\phi_1^{b\bar{a}}\left(\frac{(p_{1-}-p_{1'-})+p_{1'-}X}{p_{1-}}\right)\right]=O\left(\frac{m^2}{s}\right) \tag{3.28}$$

and the full integral (3.26) is actually $O(s^{-1})$.

A similar cancellation can be shown to apply to the set of diagrams in Fig. 24(e). In both cases the cancellations arise between pairs of diagrams related by flipping a gluon between the quark and antiquark emitted by the fast meson 1. The relative − signs in (3.26) arise just because quark and antiquark have equal and opposite colour. There is also a cancellation between Figs 24(a), (b) and (c), which can also be understood as related

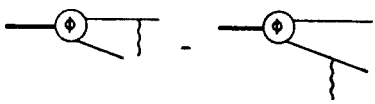

Fig. 25. Glue-flipping

to gluon-flipping, as indicated schematically in Fig. 25. These cancellations mean that the integration region (3.23) does not give a Pomeron singularity, and are $\sim s^{-1}$ at most. The cancellations do not however apply in the region (3.22), and QCD_2 does indeed exhibit Regge pole renormalization and exchange degeneracy breaking [12, 13, 70]. The model therefore realizes the ideas of Chew and Rosenzweig [69], rather than the three-trajectory suggestions of dual models and QCD_4 [35, 36].

However, the QCD colour cancellations (3.28) can be seen [12, 13] as very specific to two-dimensional kinematics. In two dimensions, the coloured quark and anticoloured quark can have no transverse separation. On the other hand Lorentz contraction allows them no longitudinal separation at high energies. Hence the colour fluxes emanating from the q and $\bar{q}$ will interfere and cancel. This would not happen in four dimensions where the q and $\bar{q}$ can separate in transverse space [67, 71]. Another way of looking at the cancellation recalls that in two dimensions there are no dynamical gluonic degrees of freedom, hence no gluonia and so no particles to be supported by a Pomeron Regge trajectory. In QCD_4, where hadrons have a transverse size, and gluonium states may exist, there is no obvious reason for cancellations like (3.28), and we may still hope that the Pomeron will exist as a third $I = 0$, $C = +1$ Regge trajectory.

3.5. Inclusive hadron reactions [12]

Many people [72] have observed an appearance of universality between final-state hadron distributions in lepton- and hadron-induced reactions. It is natural to ask whether some such effect manifests itself in QCD_2. This question can be studied using ideas similar

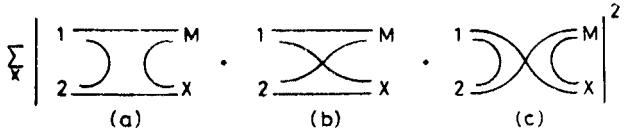

Fig. 26. Quark diagrams contributing to $\sigma(1+2 \to M+X)$

to those developed in Section 2.6 in connection with $e^+e^- \to M+X$. Consider the non-scaling $s^{\alpha_R - 1}$ Mueller-Regge [73] contribution to the hadronic inclusive reaction $1+2 \to M+X$, where some relevant quark diagrams are indicated in Fig. 26. Argumentation similar

to the e^+e^- case [9] tells us that a dominant contribution in the $1/N_c$ expansion comes from Fig. 26(a) which has direct channel resonances. Their peaks, when appropriately smeared, enhance the cross-section by a factor N_c as required by the unitarity sum rule

$$\sigma_{\text{Regge}}(1+2 \to \text{X}) = \sum_{\text{M}} \int dX_{\text{F}} X_{\text{F}} \frac{d\sigma_{\text{Regge}}}{dX_{\text{F}}} (1+2 \to \text{M}+\text{X}) \tag{3.29}$$

and the observation that the leading contribution to 2–2 meson scattering is $O(1/N_c)$.

The identity between the direct channel resonances in hadron-hadron and e^+e^- collisions suggests [12] a close relation between final state hadron distributions. Using the appropriate limit

$$m_n^2, m_3^2 \to \infty : \frac{m_{\text{X}}^2}{m_n^2} = (1-X_{\text{F}}) \text{ fixed}, \tag{3.30}$$

of the vertex function $G_{\text{MX}n}$ given in (3.2) one finds that Fig. 26(a) survives and gives

$$\frac{1}{\sigma_{\text{Regge}}(1+2 \to \text{X})} X_{\text{F}} \frac{d\sigma_{\text{Regge}}(1+2 \to \text{M}+\text{X})}{dX_{\text{F}}} = \sum_a D_{a \to \text{M}}(X_{\text{F}}), \tag{3.31}$$

where the sum runs over the quark and antiquark in the resonant state, and $D_{a \to \text{M}}(X_{\text{F}})$ was defined in Eq. (2.38).

It can be verified that the inclusive distribution (3.31) has the appropriate triple-Regge behaviour as $X_{\text{R}} \to 1$. Unfortunately the analogue of (3.31) for the scaling Pomeron contribution to inclusive hadron distributions cannot be written down in QCD_2, because of the debacle of the previous section. Therefore QCD_2 gives no reason to expect universality between scaling distributions in hadron- and lepton-induced reactions [72]. Instead a sort of convolution model [12]

$$\frac{d\sigma_{\text{Pomeron}}(1+2 \to \text{M}+\text{X})}{dX_{\text{F}}} \propto \sum_a \text{“}\left(\int_{X_{\text{F}}}^1 dY\right)\text{”} P_a(Y) D_{a \to \text{M}}\left(\frac{X_{\text{F}}}{Y}\right) \tag{3.32}$$

would seem to indicated by the diagram of Fig. 8(f), where $P_a(Y)$ is a quark probability density, given by $[\phi^{a\bar{b}}(Y)]^2$ in QCD_2, and $D_{a \to \text{M}}$ is a quark fragmentation function analogous to (2.38) in QCD_2. The integral in (3.32) is written in quotes because there must presumably be some reference to transverse degrees of freedom, and the bare Pomeron actually vanishes in QCD_2.

3.6. Conclusions

Let us finish by summarizing what has been learnt about strong interactions in studies [5–13] of QCD_2, making some remarks about the likely implications for QCD_4, and also remembering some outstanding problems to be studied in QCD_2. Going back to the various hadronic ideas listed in Section 1.2, which we have attempted to test in QCD_2, we may say the following.

Spectroscopy

Quarks indeed seem to be absent from the spectrum of QCD_2, as one might naïvely expect. There are infinite sequences of mesonic bound states, reminiscent of Regge trajectories. States made of light quarks show remnants of chiral symmetry [18], and bound states of heavy quarks show traces of charmonium [22] ideas. These topics were studied in Section 1.6.

Asymptotic freedom

The ideas of scaling with canonical behaviour resulting from free quark light-cone and short distance singularities were explicitly verified [2] in QCD_2 (see Sections 2.2 and 2.4). The long-distance confinement mechanism did not affect the perturbative "as if" calculations of the naïve parton model [25] for the reactions [3].

"Hard" processes

Some of the ideas about large momentum transfer processes not obviously related to short-distance effects worked, but others were less successful. As discussed in Section 2.5, the Drell-Yan $q\bar{q}$ annihilation model for lepton pair production in hadron-hadron collisions was verified explicitly. On the other hand, electromagnetic form factors (Section 2.3) and "large angle" elastic scattering (Section 3.3) did not work exactly as suggested by constituent interchange or hard scattering models [27, 28, 50]. The power laws were not those suggested by dimensional counting rules [29], but this feature may well be specific to two dimensions. Of more potential relevance were the renormalizations of short-distance effects by long-distance "rescattering". These effects gave the same power laws as the "bare" graphs, but would complicate attempts [27, 28] to interrelate numerically form factors and fixed angle amplitudes, if they were present in QCD_4.

"Soft" processes

As discussed in Section 3.2, the "Regge" exchanges in QCD_2 had all the properties expected [35, 36] of them in the $1/N_c$ expansion framework: factorization, duality, exchange degeneracy, etc. In addition, some interesting extra properties were found: intercepts additive in quark quantum numbers [74], a lower limit to Regge intercepts for very massive quark-antiquark trajectories, and direct as well as crossed channel factorization. On the other hand, there was found (Section 3.4) to be no new "Pomeron" singularity [31, 69] arising in $O(1/N_c^2)$ with $I = 0$ and unrelated to $q\bar{q}$ bound states. This may well be an artefact of two dimensions. Turning to inclusive reactions, we saw that universal quark fragmentation into hadrons might be true not only in deep inelastic reactions (Section 2.6) but also in hadron-hadron collisions (Section 3.5). A sort of inclusive Watson's theorem?

The above list of topics studied in QCD_2 does not mean there is nothing else to do. For a start, there are many formal questions to be resolved, such as

— the formulation and consistency of QCD_2 in other gauges [70],
— a rigorous proof of quark confinement,
— proofs of analyticity for form factors and scattering amplitudes [75].

There are also more phenomenological applications to be studied, such as
— more detailed studies [47] of heavy quark dynamics, charmonium and the like,
— mass corrections [53] to Bjorken scaling in deep inelastic scattering,
— the $\Delta I = \frac{1}{2}$ rule,
to name but a few. Also, a general study of higher order effects in $1/N_c$ would be valuable, to probe the nature of "sea" quarks, search for a Pomeron in higher orders, and see whether other lowest order $1/N_c$ results are qualitatively altered.

But the 64,000 złoty question is of course how one may use QCD_2 as a stepping stone to calculations in QCD_4. Is it useful to formulate QCD_4 on a transverse lattice [76], and use QCD_2 results as an input to higher order calculations? Is it profitable to pursue the analogy of QCD_2 to a string model [17] in higher dimensions? Is it possible to reformulate the naive covariant parton models so as to incorporate [77] the lessons learnt about quark confinement in QCD_2? Can one construct any sort of $2+\varepsilon$ [78] expansion for QCD? I don't know.

Much of this review is based on work done in collaboration with Rich Brower, Michael Schmidt and Joe Weis. I am very grateful to them, and Marty Einhorn for many discussions. It is also a pleasure to thank Jochen Kripfganz, Jack Paton, Chris Sachrajda, Gabriele Veneziano and T. T. Wu for discussions and comments on the manuscript.

REFERENCES

[1] Anonymous — private communication.
[2] H. D. Politzer, *Phys. Rep.* **14C**, 129 (1974).
[3] G. Preparata rightfully emphasizes this criticism of QCD phenomenology. For an alternative approach to quark dynamics, see G. Preparata, N. Craigie, *Nucl. Phys.* **B102**, 478 (1976); N. Craigie, G. Preparata, *Nucl. Phys.* **B102**, 497 (1976).
[4] For a comprehensive review, see W. Marciano, H. Pagels, *Quantum Chromodynamics — a review*, Rockefeller preprint COO-2232B-130, 1977.
[5] G. 't Hooft, *Nucl. Phys.* **B75**, 461 (1974).
[6] For related studies in QED_2, see for example A. Casher, J. Kogut, L. Susskind, *Phys. Rev.* **D10**, 732 (1974).
[7] C. G. Callan, N. Coote, D. J. Gross, *Phys. Rev.* **D13**, 1649 (1976).
[8] M. B. Einhorn, *Phys. Rev.* **D14**, 3451 (1976).
[9] M. B. Einhorn, *Phys. Rev.* **D15**, 3037 (1977).
[10] R. C. Brower, J. Ellis, M. G. Schmidt, J. H. Weis, *Phys. Lett.* **65B**, 249 (1976); M. B. Einhorn, S. Nussinov, E. Rabinovici, *Phys. Rev.* **D15**, 2282, (1977).
[11] J. Kripfganz, M. G. Schmidt, *Nucl. Phys.* **B125**, 323 (1977).
[12] R. C. Brower, J. Ellis, M. G. Schmidt, J. H. Weis, *Nucl. Phys.* **B128**, 131, 175 (1977).
[13] M. B. Einhorn, E. Rabinovici, *Nucl. Phys.* **B128**, 421 (1977).
[14] It may be that quarks are not completely confined in the real world — see G. S. LaRue, W. M. Fairbank, A. F. Hebard, *Phys. Rev. Lett.* **38**, 1011 (1977). However, the quark liberation threshold is presumably at rather high energies, and below that threshold the phenomenology is probably very similar to the usual idealization of complete confinement. There seems to be no inconsistency known between QCD_4 and quark liberation. It is possible that QCD_4 with massless gluons does not in fact confine, and presumably QCD_4 with massive gluons would allow quarks to get out. For a comprehensive study of these questions, see A. De Rújula, R. G. Giles, R. L. Jaffe, MIT preprint CTP 635, 1977.

[15] There is no conclusive hint of confinement from perturbation theory in QCD_4 — see C. T. Sachrajda, Lectures at this School.

[16] It has been suggested that non-perturbative effects related to instantons may confine quarks — see A. M. Polyakov, *Nucl. Phys.* **B120**, 429 (1977). This suggestion has not yet borne fruit — see G. 't Hooft, Utrecht University preprint *Some Observations on Quantum Chromodynamics*, 1977. The instanton and $(1/N_c)$ approaches to confinement are rather orthogonal.

[17] P. Goddard, J. Goldstone, C. Rebbi, C. B. Thorn, *Nucl. Phys.* **B56**, 109 (1973); C. Rebbi, *Phys. Rep.* **12C**, 1 (1974).

[18] For a review, see S. Weinberg, *Lectures on Elementary Particles and Quantum Field Theory*, 1970 Brandeis Summer Institute, Ed. by S. Deser, M. Grisaru and H. Pendleton, MIT Press, Cambridge, 1971.

[19] See for example S. Weinberg, *Phys. Rev.* **D11**, 3583 (1975). Recently it has been proposed that instantons may also solve this problem: G. 't Hooft, *Phys. Rev. Lett.* **37**, 8 (1976) and *Phys. Rev.* **D14**, 3432 (1976). This suggestion may also not yet have borne fruit: R. J. Crewther, *Phys. Lett.* **70B**, 349 (1977).

[20] S. L. Adler, *Phys. Rev.* **137**, B1022 (1965).

[21] A. Chodos, R. L. Jaffe, K. Johnson, C. B. Thorn, V. F. Weisskopf, *Phys. Rev.* **D9**, 3471 (1974); L. Susskind, *Coarse-grained Quantum Chromodynamics.* Lectures at the 1976 Les Houches Summer School, Yeshiva University preprint, 1977.

[22] T. Appelquist, H. D. Politzer, *Phys. Rev. Lett.* **34**, 43 (1975), and *Phys. Rev.* **D12**, 1404 (1975).

[23] T. Appelquist et al., *Phys. Rev. Lett.* **34**, 365 (1975); E. Eichten et al., *Phys. Rev. Lett.* **34**, 369 (1975).

[24] For a review, see J. Ellis, *Deep Hadronic Structure* — Lectures at the 1976 Les Houches Summer School, CERN preprint, 1977.

[25] R. P. Feynman, *Photon-Hadron Interactions*, Benjamin, Reading 1972.

[26] S. D. Drell, T.-M. Yan, *Phys. Rev. Lett.* **24**, 855 (1970).

[27] For a review, see D. Sivers, S. J. Brodsky, R. Blankenbecler, *Phys. Rep.* **23C**, 1 (1976).

[28] For a short-distance approach to "hard" processes, see S. J. Brodsky, Lectures at this School.

[29] S. J. Brodsky, G. Farrar, *Phys. Rev. Lett.* **31**, 1153 (1973) and *Phys. Rev.* **D11**, 1309 (1975); V. A. Matveev, R. M. Muradyan, A. N. Tavkhelidze, *Lett. Nuovo Cimento* **7**, 719 (1973).

[30] R. Dolen, D. Horn, C. Schmid, *Phys. Rev.* **166**, 1768 (1968).

[31] P. G. O. Freund, R. J. Rivers, *Phys. Lett.* **29B**, 510 (1969); P. G. O. Freund, *Lett. Nuovo Cimento* **4**, 147 (1970).

[32] As realized for example in the Veneziano model: G. Veneziano, *Nuovo Cimento* **57A**, 190 (1968).

[33] An early prophet was H. Lipkin, Les Houches Summer School, 1968, ed. C. De Witt and V. Gillet, Gordon and Breach, New York 1969, p. 585.

[34] G. 't Hooft, *Nucl. Phys.* **B72**, 461 (1974).

[35] G. Veneziano, *Nucl. Phys.* **B117**, 519 (1976).

[36] G. Veneziano, Talk given at the XIIth Rencontre de Moriond, Flaine 1977 — CERN preprint TH. 2311, 1977.

[37] For brave attempts, see M. Dorgut, *Nucl. Phys.* **B116**, 233 (1976); G. C. Rossi, G. Veneziano, *Nucl. Phys.* **B123**, 507 (1977). Unfortunately, these authors have not found a systematic expansion parameter as unimpeachable as $1/N_c$.

[38] *Dual Theory*, ed. M. Jacob, North-Holland, Amsterdam, 1974.

[39] Gluonium is not excluded by $\pi\pi$ phase shifts, for example. You may be titillated by the recent analysis of $\pi\pi$ scattering due to A. D. Martin, M. Pennington, CERN preprint TH. 2353, 1977.

[40] There are serious problems of consistency when QCD_2 is formulated in other gauges — see Y. Frishman, C. T. Sachrajda, H. D. I. Abarbanel, R. Blanckenbecler, *Phys. Rev.* **D15**, 2275 (1977); N. Pak, H. C. Tze, *Phys. Rev.* **D14**, 3472 (1976); A. J. Hanson, R. D. Peccei, M. K. Prasad, *Nucl. Phys.* **B121**, 477 (1977); A. Patrascioiu, San Diego preprint UCSD 10P10-170, 1977;

A. J. Hanson, M. K. Prasad, Lawrence Berkeley Laboratory preprint LBL-6117, 1977. T. T. Wu, CERN preprint TH. 2366 (1977).

[41] This prescription was first used by Y. Frishman, CERN preprint TH. 2039, 1975, unpublished.

[42] For a complete discussion and clarification of the literature, see M. B. Einhorn — Ref. [8].

[43] W. A. Bardeen, I. Bars, A. J. Hanson, R. D. Peccei, *Phys. Rev.* **D13**, 2364 (1976); I. Bars, *Phys. Rev. Lett.* **36**, 1521 (1976), and the third and fourth papers in Ref. [40].

[44] H. Leutwyler, *Phys. Lett.* **48B**, 431 (1974).

[45] A. W. Smith, DAMTP, Cambridge, preprint 76/17, 1976.

[46] S. Coleman, *Comm. Math. Phys.* **31**, 259 (1973).

[47] See also the third paper in Ref. [40]. I thank J. E. Paton for discussions on the non-relativistic bound state limit in QCD_2.

[48] J. Ellis, *Phys. Lett.* 35**B**, 537 (1971); J. D. Stack, *Phys. Rev. Lett.* **28**, 57 (1972); H. Fritzsch, P. Minkowski, *Nucl. Phys.* **B55**, 363 (1973); J. Ellis, Y. Frishman, *Phys. Rev. Lett.* **31**, 139 (1973).

[49] P. V. Landshoff, J. C. Polkinghorne, *Phys. Rep.* **5C**, 1 (1972); See also Refs [27] and [28].

[50] I thank Stan Brodsky for many fascinating discussions about this and related issues which greatly deepened my awareness of my ignorance.

[51] S. D. Drell, T.-M. Yan, *Phys. Rev. Lett.* **24**, 181 (1970); G. West, *Phys. Rev. Lett.* **24**, 1206 (1970).

[52] H. D. I. Abarbanel, M. L. Goldberger, S. B. Treiman, *Phys. Rev. Lett.* **22**, 500 (1969).

[53] H. Georgi, H. D. Politzer, *Phys. Rev. Lett.* **36**, 1281 (1976), Erratum *Phys. Rev. Lett.* **37**, 68 (1976), and *Phys. Rev.* **D14**, 1829 (1976). For comments on this analysis, see R. K. Ellis, R. Petronzio, G. Parisi, *Phys. Lett.* **64B**, 97 (1976); R. Barbieri, J. Ellis, M. K. Gaillard, G. G. Ross, *Phys. Rev.* **64B**, 171 (1976) and *Nucl. Phys.* **B117**, 50 (1976); D. J. Gross, S. B. Treiman, F. A. Wilczek, *Phys. Rev.* **D15**, 2486 (1977). For comments on these comments, see A. de Rújula, H. Georgi, H. D. Politzer, *Phys. Rev.* **D15**, 2495 (1977).

[54] R. L. Jaffe, *Phys. Lett.* **37B**, 517 (1971), *Phys. Rev.* **D5**, 2622 (1972); J. C. Polkinghorne, *Nuovo Cimento* **8A**, 572 (1972).

[55] See however C. T. Sachrajda CERN preprint TH. 2416, 1977.

[56] C. E. DeTar, S. D. Ellis, P. V. Landshoff, *Nucl. Phys.* **B87**, 176 (1975).

[57] See for example H. Satz — Lectures at this School.

[58] J. B. Kogut, *Phys. Lett.* **65B**, 377 (1976); I. Hinchliffe, C. H. Llewellyn Smith, *Phys. Lett.* **66B**, 281 (1977).

[59] This power behavior can perhaps be thought of as reflecting a "Reggeization" of the quark.

[60] In addition to this "Regge" pole, there is also a fixed pole at $J = -1$, which is actually leading for $\beta_f + \beta_d > 1$ and is required for the analyticity of the forward elastic $2-2$ meson amplitude.

[61] R. Blankenbecler, S. J. Brodsky, *Phys. Rev.* **D10**, 2973 (1974).

[62] R. C. Brower, C. T. Sachrajda and I may have some arguments to support this possibility in QCD_4.

[63] B. Schrempp, F. Schrempp — private communication.

[64] This property would seem natural in 4 dimensions if one were prepared either to invoke super-local duality, of if one adopted a naive valence-only approximation to the quark content of mesons.

[65] J. D. Bjorken, J. B. Kogut, *Phys. Rev.* **D8**, 1341 (1973).

[66] T. T. Wu, C. N. Yang, *Phys. Rev.* **137**, B708 (1965).

[67] F. E. Low, *Phys. Rev.* **D12**, 163 (1975); S. Nussinov, *Phys. Rev. Lett.* **34**, 1286 (1975) and *Phys. Rev.* **D14**, 246 (1976).

[68] Dual models [38] have $\alpha'_P = \frac{1}{2}\alpha'_P$, QCD_4 models have trajectories with slopes 1/2 and/or 2/3 α'_P, the ISR finds α'_P somewhat $< \frac{1}{2}\alpha'_P$.

[69] G. F. Chew, C. Rosenzweig, *Nucl. Phys.* **B104**, 290 (1976).

[70] The other $O(1/N_c^2)$ graphs also renormalize Regge singularities and generate Regge "cuts" in the ways expected on the basis of $1/N_c$ expansions [35] and dual models [38]. See Ref. [12] for more details.

[71] For a model for how this may happen, see J. F. Gunion, D. E. Soper, *Phys. Rev.* **D15**, 2617 (1977).

[72] Some studies were mentioned in Ref. [18] of the second paper of Ref. [12]. Recent investigations

include: B. Andersson, G. Gustafson, C. Peterson, *Phys. Lett.* **69B**, 221 (1977); J. Dias de Deus, S. Jadach, *Phys. Lett.* **70B**, 73 (1977).

[73] A. H. Mueller, *Phys. Rev.* **D2**, 2963 (1970); G. Altarelli, R. A. Brandt, G. Preparata, *Phys. Rev. Lett.* **26**, 42 (1971).

[74] Other derivations of this property were made in the early days of the Veneziano model. See for example M. Ademollo, G. Veneziano, S. Weinberg, *Phys. Rev. Lett.* **22**, 83 (1969).

[75] R. C. Brower, W. L. Spence, J. H. Weis, University of Washington preprint (1977), have recently made progress in proving analyticity for electromagnetic form factors.

[76] W. A. Bardeen, R. B. Pearson, *Phys. Rev.* **D14**, 547 (1976).

[77] M. B. Einhorn, G. C. Fox, *Nucl. Phys.* **B89**, 45 (1975).

[78] One idea doing this has been considered by R. C. Brower and W. L. Spence — private communication.